

5. Nonlinear and hysteretic models for masonry

The modelling of masonry traditionally falls into two distinct classes [1]:

(i) the discrete or micromechanical models accounting for the morphology of masonry, so that each basic masonry constituents are considered separately. This approach refers as well to simplified models where some constituents are omitted or combined. The micro-mechanical approach is in principle the best modelling scale to understand the salient features of the in-plane behaviour of masonry panels. However, such modelling cannot reasonably be applied to deal with structure larger than a single wall.

(ii) the macro-mechanical models (also called homogeneous or continuous models) account for the behaviour of a typical relevant unit cell by establishing a direct constitutive law between the average stress and strain states [2]. Such a relationship can be obtained either by using homogenisation techniques, or assimilating experimental data. When constitutive models contribute to the prediction of the dynamic response, the second option is usually preferred.

However arbitrary it may appear, we shall also draw a distinction between models conceived to be applied in static analyses and models that operate in dynamics. The clean methodological differences in the present literature still justify splitting-up the chapter into two distinct sections about static and dynamic models, respectively.

5.1 Constitutive models for static analysis

In this paragraph, a review of the principal constitutive models for simulating the behaviour of masonry subject to in-plane cyclic loading is presented. In accordance with the given classification, models are divided into discrete and continuous models.

5.1.1 *Discrete models*

The discrete approach generally resorts to different elements for modelling the entities which compose the masonry. Such an approach is mostly used in cases that require higher level of detail because of its computational complexity. In its complete version, the bricks and the mortar joints are modelled by using continuous elements, the interfaces between bricks and joints are modelled by using discontinuous elements. In the

past a simplified approach was also pursued by condensing the interface and the mortar joint elements into a single interface element. An interface element is an element which allows for discontinuities in the displacement fields and its behaviour is described by tension-displacement relationships between the two opposite faces.

The first type of discrete model was proposed by Page in 1978 [3] using some experimental evidences as assumptions:

- bricks exhibit an elastic-brittle behaviour;
- the mortar has a highly nonlinear behaviour;
- masonry as a whole has a good capability to carry compression loads and the maximum tensile stress governs the compression failure due to splitting phenomena;
- the tensile strength of the masonry is limited to the poor cohesion between mortar and bricks;
- most of the inelastic deformations is concentrated at the mortar joints.

Therefore, masonry is modelled as a collection of elastic elements (bricks) connected by mortar joints, where all of the nonlinearities of the global behaviour are concentrated. Consequently, two main types of damage mechanism are considered for mortar joints: a tensile or a shear failure. Until one of these two cases happens, the joints are supposed to retain an elastic behaviour. Such an approach often requires a finite element model of the masonry, e.g. using elastic shells to describe the bricks and interface elements to represent mortar joints. Page [3] conducted a few experimental campaigns in order to characterise the elastic and inelastic parameters of the materials used for the elements. This was the first model capable to describe the progression of the damage of masonry under loading; all the damage was concentrated assuming degradation in the stiffness of the interface.

Another important example of discrete modelling is the interface model proposed by Lofti and Shing [4]. It is worth noticing that in this case the focus of the model is the characterisation of the behaviour of masonry panels under combined axial and shear loads (like in the case of seismic actions). In accordance with the above mentioned Page model, the bricks retain an elastic behaviour and damage may occur only in the mortar joints. In this mode, two different damage mechanisms are considered: shear failure and tensile failure. Differently from the Page model, the stiffness matrix in this case does not undergo modification during the loading history: damage does not modify the stiffness system. The failure criteria proposed by the interface model is a nonlinear combination of a Mohr-Coulomb criteria with a cut-off tensile rupture criteria, resulting in a hyperbolic domain. This interface model allows computing the ultimate load of the structure and to characterise its principal collapse mechanisms and damage localisation.

Baggio and Trovalusci [5] studied the behaviour of masonry shear walls, with particular emphasis on historic masonry, which typically shows inferior quality mortar. In such a case, the masonry is characterised by inhomogeneity, anisotropy, poor and scattered tensile strength. This study analysed the influence of the disposition of the blocks in the wall rather than the cohesive property of the mortar (in some examples of historic masonry, mortar is not even present). The authors used the FE method to develop a model which considered blocks as rigid elements, so as to be replaced by constraint equations. This assumption has been inferred from rock mechanics, because deformability is assumed to be concentrated in the weaker part of the masonry (joints). On the other hand, contact surfaces were meshed by using interface elements able to withstand

compression forces only, in the direction normal to the surfaces, and to shear forces in the other direction. Shear resistance was modelled by using a Coulomb's law. The influence of the disposition of the block has been introduced by the mesh of the FE method. One of the important remarks is that, whilst the model showed good capability to evaluate the ultimate strength of the walls, with the increasing size of the problem, a continuum model capable to take into account the geometrical structure should be preferred.

Lourenco and Rots [6] introduced a model with relevant innovations with respect to previous discrete models. In fact, for the first time different failure mechanisms such as the rupture of the blocks were taken into account. In detail, the model considers the following damage mechanisms:

- failure of the mortar joints for tensile stresses;
- sliding of mortar joint for shear stress, for low values of compression;
- failure of blocks for tensile stress induced by deformation of mortar joints;
- failure of blocks for shear stress, when the compression applied to mortar joints is enough to limit the sliding;
- failure of blocks for splitting mechanism, when high values of compression normal to the plane of mortar joints are present.

Also in this model, the blocks are seen as continuous elements and the damage is concentrated at the interface elements. The difference is that, in this case, interface elements are present not only in between blocks, where mortar joints are located, but also in the middle of blocks (where potential cracks of blocks may occur). The two interface elements are characterised by two different laws. In the case of mortar joints an elasto-plastic law is used, limited by different criteria for each failure mechanisms involving mortar: the limit surface evolves with a softening-type law which includes damage mechanism for tension, shear and compression. These three damage mechanisms are ruled by different criteria: a cut-off criterion for stress, a Coulomb criterion for sliding with friction and a cap model for compression failure. On the other hand, the interface in-between blocks is characterised by a tensile failure model with softening behaviour. Also in this case, as in previously mentioned models, the damage of the material is described in terms of a decrease in strength and not in stiffness.

Giambanco *et al* [7] recently proposed a discrete model for composite materials which shares most of the characteristics of the previous models (it does not allow for block cracks). What is interesting about this model is the interface law, which is developed in the framework of elasto-plasticity for non-standard materials and particular attention is paid to the cohesive-frictional joint transition. In fact, the formation of a rough fracture surface is considered and a friction law describes the evolution of the contact surface. The introduction of a rough contact surface produces, at the joint level, effects such as geometrical dilatancy and an increase in the residual shear strength.

Another possible approach is the one proposed by Chetouane *et al* [8] who used the Discrete Element method in order to simulate a masonry structure considered as a collection of rigid or deformable blocks, interacting together by contact laws. The non-smooth contact dynamics (NSCD) resolution method is used for the modelling of granular media. The average local strain and stress tensors are defined on an elementary cell. A rigid approach is faster than a deformable one but less realistic. The dispersion of the results of the average stress tensor can be reduced when averaging this tensor on more than one block. The stress tensor averaged on all the assembly of blocks has a constant

value independent of the type of the approach but function of the geometry, the loads applied to the structure, the mechanical and physical properties of the blocks.

5.1.2 Continuous models

The continuous approach may be used when the analysed portion of the structure is large enough to allow local stress to be considered homogeneous, without a need for distinguish between joints and blocks.

In literature there exist various proposal for constitutive laws conceived for continuous models. Again, two approaches can be distinguished: phenomenological approaches, which are mostly based on experimental evidences and the macroscopic behaviour of masonry, and homogenisation approaches, which consider masonry as a composite material with periodic structure. Whilst the first type of approach is more used in limit analysis, the latter seems more suited for the study of the material undergoing damage.

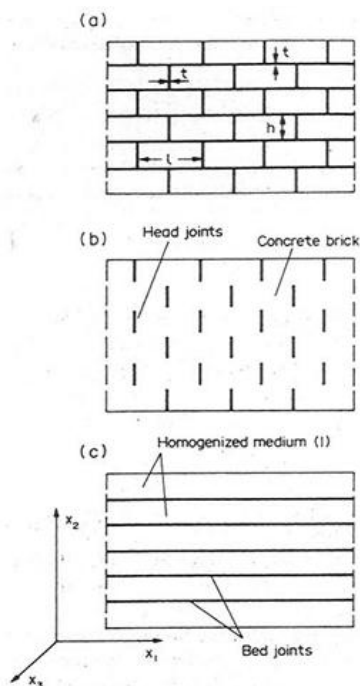


Figure 5.1 - Two steps homogenisation as proposed by Pietruszczak and Niu [9].

One of the most important contributions to the continuous modelling of masonry is due to Pietruszczak and Niu [9]. They proposed a model suitable for three-dimensional modelling of the structure, based on a micromechanical approach, where masonry is considered as a two-phase composite material: a matrix of blocks intersected by two

groups of mortar joints orthogonal with respect to each other. The homogenisation procedure is conducted in two different steps (see figure 5.1): in the first step (b), a continuum composed of the block matrix is homogenised with the secondary mortar joints, considered as inclusions. Pietruszczak and Niu assumed an elasto-brittle behaviour of the joints and then proceeded with the second step (c), homogenising also the principal mortar joints, in this case considered to behave in an elasto-plastic fashion. Only two failure scenarios have been contemplated: failure of the block matrix or of the principal mortar joints. Therefore, the continuum so obtained behaves as an elastic orthotropic material, imposing a failure criterion for the blocks. For what concerns the mortar joints, a Coulomb friction law is suitable to describe the failure criteria of these elements.

Maier *et al* [10] proposed an alternative model which works in the other way around the problem: the mortar is considered the matrix of a composite material, and the blocks are considered reinforcement inclusions to the material. Both phases are considered isotropic, elastic and interfaces must bond perfectly. Also in this case the homogenisation is performed in two different steps: a strip of secondary mortar joints and blocks in the first step and a strip of primary joints and blocks in the second step. In this model, the behaviour of the blocks is assumed to be elasto-brittle. The mortar matrix is considered to behave as an elastic material subject to damage.

Another relevant example is the micro-structural model proposed by Alpa e Monetto [11]. The model aims at modelling the behaviour of masonry panels subject to in-plane loading. This model assumes a dry masonry: in such a case the geometry of the blocks plays a pivotal role in the overall behaviour of the panel. In this case the material of the blocks is assumed to be linear elastic with plane and stable micro-cracks. The joints are considered as macro-cracks. The collapse criterion is assumed to be when the sliding of the joint is inelastic and uncontrolled. On the basis of these considerations, four different collapse mechanisms were considered, involving both primary and secondary joints. Probably, the most important characteristic of the model is the dependence of the resistance domain on the masonry pattern.

Another model that is suited for evaluating the collapse of masonry panels subject to in-plane loadings is due to De Buhan and De Felice [12] and has a domain similar to the Alpa Monetto. This model allows also for tensile stresses.

An example of model for historic masonries characterised by period structure is the one proposed by Luciano and Sacco [13]. In old masonries the strength of the mortar can be usually be assumed to be much lower than the strength of the blocks. Therefore this model assumed that fractures can develop only within the mortar material, which behaves in a perfect elastic-brittle manner. Moreover, because the mortar thickness is small, cracks may develop only vertically and horizontally (parallel to the joint direction). On the other hand, the bricks are assumed to behave indefinitely elastic. The elementary cell defined in figure 5.2 allows for 8 different state of damage (with the assumption that damage can occur only in mortar joints). Considering that damage is irreversible, the succession of the different state of damage through damage history is limited to a finite number of combinations. The homogenised material has varying characteristics for each damage state; in fact, by modifying the global elastic modulus of the material one can achieve a representation of the damage.

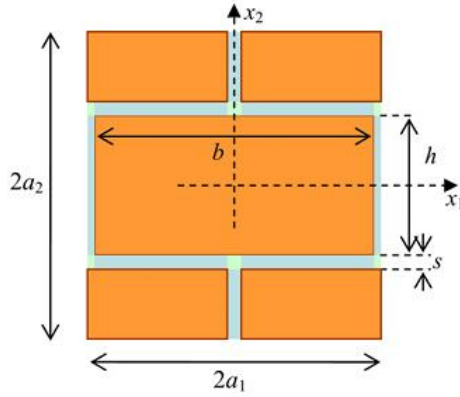


Figure 5.2 - Repetitive unit cell for the masonry material [14].

Sacco also proposed a more general model than the above mentioned model in [14]. In this paper Sacco resorts to a micromechanical analysis which takes in account the strong nonlinear response of masonry constituents. Also in this case, the constitutive law for bricks element is a linear elastic relationship. For what concerns the mortar, an interface mechanical model was developed ad hoc. The constitutive law accounts for the coupling of the damage and friction phenomena occurring in the mortar joints during the strain history: whilst a linear elastic constitutive law is adopted for the undamaged part of the representative mortar element, a Coulomb friction law is considered in the damaged part of it.

Lourenco *et al* [15] proposed a different model allowing for the representation of plane masonries subject to generic loadings. In this case the model is formulated as an in plane stress model for quasi-brittle orthotropic materials. The following failure criteria are assumed: the Hill criterion for compression and a modified Rankine criterion for tension (Figure 5.3). The damage evolution laws, involving both stiffness and strength, are defined by using energy criteria typical of fracture mechanics. This model does not distinguish among different damage mechanisms but employs macroscopic continuum damage laws calibrated on the basis of experimental evidences.

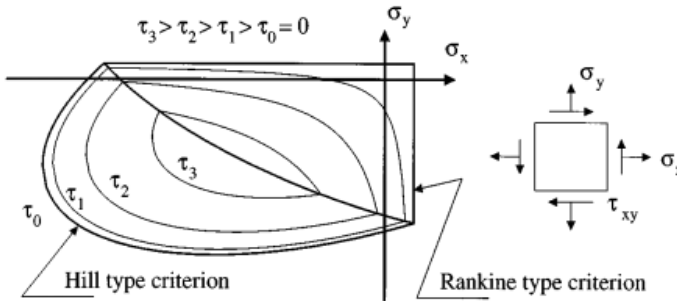


Figure 5.3 - Failure domain proposed by Lourenco [15].

Gambarotta and Lagomarsino presented in two companion papers [16,17] a constitutive law aimed to the evaluation of the lateral response of in-plane loaded masonry shear walls patterns (i.e. seismic actions). The continuum model is based on the assumption of an equivalent stratified medium made up of layers representative of the mortar bed joints and of the brick units and head joints, respectively. The mechanic discontinuity of secondary mortar joints is not considered in this model. Three different damage mechanisms are considered: failure of principal mortar joints (associated to tensile stress acting orthogonally at their plane), failure of principal mortar joints for tangential friction, failure of the blocks for compression or shear effects (see figure 5.4a).

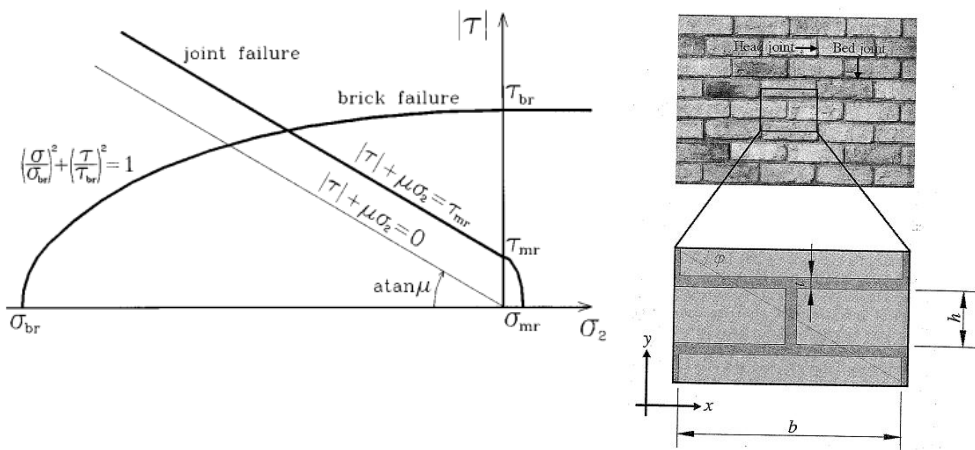


Figure 5.4 - (a) Mortar joints and block failure domains [17]. (b) Reference volume for Calderini and Lagomarsino [18].

Calderini and Lagomarsino proposed in [19,18] a further generalisation of the Gambarotta - Lagomarsino model by taking in account also the secondary mortar joints. The elementary cell chosen in this homogenisation approach is the one shown in figure 5.4b. In the end a formulation for an anisotropic continuum damage model was achieved. The model is quite simple but still able to capture the main in-plane damage mechanisms of masonry. The fabric of masonry is described by only one parameter: the angle of interlocking. The resisting mechanisms of the material are based on both damage and friction laws, and the parameters involved are inferred by experimental data.

A homogenisation approach was proposed by Cluni and Gusella [20] by using the concept of period cell and extending it to the concept of representative volume element. The authors also states that, even though for old type of masonries it is quite difficult to identify a periodic cell, due to the general irregular pattern, the material can be still define as quasi-periodic. The authors proposed an iterative optimisation process in order to determine the representative volume element by using a rectangular test window.

Massart *et al* [21] proposed a mesoscopic study in order to introduce anisotropy in macroscopic models. It was highlighted by the authors that under plane stress assumption, a scalar damage meso-model allows for obtaining realistic in-plane damage patterns. Both the materials for brick and mortar are considered to be isotropic. The

model assumes that the interface between constituents is perfect and the effect of the interface failure is incorporated in a modification of the tensile characteristics of mortar. The model preserves compressive strength and bulk material properties of the mortar. For what concerns damage laws, whilst a modified von Mises criterion was chosen for bricks, a Coulomb friction law was used for mortar.

Wu and Hao [22] proposed a homogenisation technique for the derivation of 3D masonry properties, therefore considering also out-of-plane properties. The model is particularly focused on masonry structures subject to blasting loads. In this case, the homogenised model was realised by using the material properties such as threshold tensile strains and yield surface, using these data to characterise and elastoplastic anisotropic incremental matrix. Four different failure behaviours characterise the homogenised material: tensile failure, shear failure, compressive failure and high pressure failure.

Quinteros *et al* [23,24] proposed another homogenisation method based on a different unit cell (see figure 5.5). The model is particularly simplified in order to save on computational time and to simplify the mesh generation process, and the number of elements needed is much smaller than in macromodels. A linear elastic constitutive law is considered for the bricks, while the unilateral damage model is implemented for the mortar in order to describe the behaviour of brittle materials subjected to alternating tension-compression cyclic loads, by introducing two scalar damage variables. In the end, the anisotropic behaviour is reproduced by recurring to an orthotropic constitutive tensor for the masonry.

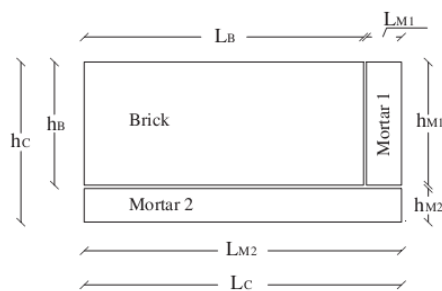


Figure 5.5 - Unit cell as proposed by Quinteros *et al* [23].

Cecchi and Sab [25] presented a homogenisation approach applied to orthotropic 3D periodic plates. The theory of Caillerie [26], which leads to a homogeneous Love-Kirchhoff model, has been extended by Cecchi and Sab in order to take into account the shear effects for thick plates. A homogenised Reissner-Mindlin plate model has been proposed. Hence, the determination of the shear constants requires the resolution of an auxiliary 3D boundary value problem on the unit cell that generates the periodic plate. This homogenisation procedure has been proposed to be applied to periodic brickwork panels. This model is focused on the simulation of out-of-plane forces.

The same authors, Cecchi and Sab [27], proposed both a discrete and a continuous model for in plane loaded non-periodic masonries (typically historic masonries), by means of a perturbation approach and to evaluate the effect of a random perturbation on the elastic response of a periodic masonry wall. The random masonry is obtained starting

from a periodic running bond pattern. A random perturbation on the horizontal positions of the vertical interfaces between the blocks which form the masonry wall is introduced. In this way, the height of the blocks is uniform, while their width in the horizontal direction is random. The perturbation is limited such as each block has still exactly 6 neighbouring blocks. In a first discrete model, the blocks are modelled as rigid bodies connected by elastic interfaces (mortar thin joints). In other words, masonry is seen as a “skeleton” in which the interactions between the rigid blocks are represented by forces and moments which depend on their relative displacements and rotations. A second continuous model is based on the homogenization of the discrete model. Explicit upper and lower bounds on the effective elastic moduli of the homogenized continuous model are obtained and compared to the well-known effective elastic moduli of the regular periodic masonry. It is found that the effective moduli are not very sensitive to the random perturbation (less than 10%). At the end, the Monte Carlo simulation method is used to compare the discrete random model and the continuous model at the structural level (a panel undergoing in plane actions). The randomness of the geometry requires the generation of several samples of size L of the discrete masonry. For a sample of size L , the structural discrete problem is solved using a previously proposed discrete model [28] and the average solution over the samples gives an estimation which depends on L . As L increases, an asymptotic limit is reached. One issue is to find the minimum size for L and to compare the asymptotic average solution to the one obtained from the continuous homogenized model.

Phenomenological approaches have been investigated too, such in the case of the model proposed by Andreaus [29]. Also in this case the model aims to describe the behaviour of masonry panels subject to in-plane loads. An orthotropic elastic model is calibrated by using experimental evidences. Three main collapse mechanisms are adopted, in this case: sliding along the principal mortar joints (by using a modified Mohr-Coulomb friction law), splitting collapse mechanism (for tensile stresses) and a compression collapse mechanism.

5.2 Constitutive models for dynamic analysis

Modelling of the nonlinear behaviour of systems subject to seismic excitation has always been a topical issue of earthquake engineering. In this section, a more general class of models aimed to simulate the seismic response of dynamic systems will be analysed. In fact, when structures are dynamically excited beyond yield point (as happens during strong earthquake motion) they typically show an evolutive and hysteretic behaviour.

The most challenging problem with constitutive models for dynamic analysis is dissipation. In fact, whatever is the type of structure and the material, relevant information about damping comes from experimental tests. The consequence is that, to date, the vast majority of models accounting for damping require a phenomenological approach, whence the importance of dynamic testing and identification (see chapter 7).

5.2.1 Hysteretic models and operators

A model (or operator) may be defined as a relationship between an input (time-) function $u(t)$ and an output (time-) function $f(t)$. For structural systems, the input function often is a displacement or a rotation, while the output function usually is a force or a moment. Hysteresis operators are a particular class of operators characterized by (i) causal memory and (ii) rate-independence [37]. The first property can be explained by the following expression:

$$f(t) = \mathfrak{R}\left(u(\tau)\Big|_{\tau \in [0,t]}, f_0\right)(t) \quad (5.1)$$

where t is the current time, τ is the generic time, $u(t)$ is the input function, $f(t)$ is the output function with initial value f_0 , \mathfrak{R} is the operator. The above equation states that the output r at the current time t depends on the past input history $u(\tau)$ with $0 \leq \tau \leq t$. A model fulfilling equation (5.1) is said to possess causal memory. The past history dependence implies that the standard restoring force function $f = f(x, \dot{x})$ is not single-valued, i.e. for given values of u and \dot{u} , several different values of r may occur, according to the past input history. Conversely, the function f associated with the following differential formulation

$$\dot{f} = g(\dot{x}, f) \quad (5.2)$$

is single-valued, even though it defines a history-dependent force f . Causality follows from the differential formulation, while memory is associated with the presence of f as state variable in the function g .

The second distinctive property of a hysteresis operator, the rate-independence, can be explained by using the notion of hysteresis diagram, i.e. the input vs. output parametric plot $(x(t), f(t))$. For hysteretic models, the hysteresis diagram does not change when the rate of the input $\dot{x}(t)$ (or equivalently, the time scale) changes. In other words, hysteresis loops do not change when the time-scale changes. For models defined by the differential equation (5.1), rate-independence occurs if and only if the function g is positively homogeneous of order one with respect to the variable \dot{x} :

$$g(k\dot{x}, f) = k \cdot g(\dot{x}, f) \quad (5.3)$$

for all $k > 0$. A further generalization of equation (5.1) reads:

$$\dot{f} = g(\dot{x}, f, x) \quad (5.4)$$

Equation (5.4) defines a so-called Duhem model [37]. Memory, causality and rate-independence definitions are the same as for the model in equation (5.1).

The well-known Bouc-Wen model [24, 25] is a particular case of equation (5.1):

$$\dot{f} = A \dot{x} - \beta f |f|^{n-1} |\dot{x}| - \gamma |f|^n \dot{x} \quad (5.5)$$

For this model, rate-independence can be easily proven using equation (5.5). Moreover, the differential expression implies causality, while the presence of f as state variable in the function g entails a memory effect. The role of f can also be described by writing equation (5.6) in a different form:

$$\begin{aligned} f &= f(x, x^p) = A(x - x^p) \\ \dot{x}^p &= \beta(x - x^p) \left| A(x - x^p) \right|^{n-1} |\dot{x}| - \frac{\gamma}{A} \left| A(x - x^p) \right|^n \dot{x} \end{aligned} \quad (5.6)$$

where x^p is an internal variable with the physical meaning of inelastic (or plastic) part of the total displacement x .

The number of internal variables is sometimes called “dimension of the memory” [37]. In summary, the Bouc-Wen model is hysteretic, since it has causal memory (of dimension 1) and is rate-independent. This model will be used here after as reference hysteretic model.

For comparison purposes, observe that the linear elastic model $f(t) = A \cdot x(t)$ is rate-independent, since the parametric plot $(x(t), f(t))$ is the line with slope A for any time-scale. Alternatively, notice that the rate form of this model, i.e. $\dot{f} = A \cdot \dot{x}$ is characterised by a function $f = f(\dot{x}) = A \cdot \dot{x}$ which is positively homogeneous of order one. This linear model has zero memory, since only the current value of the input, i.e. $x(t)$, affects the output. Therefore, it is not hysteretic. Another interesting example is the Maxwell model $f = A \cdot \dot{x} - \beta \cdot f$. It is causal with memory, but it is rate-dependent, as it can be easily verified by applying equation (5.2): it is not a hysteretic model.

One may further classify hysteretic models in two categories of models, based on their analytical formulation: piecewise-linear hysteretic models and curvilinear hysteretic models. The first ones are characterised by relatively simple constitutive equations, sharp yield transitions and linear relationship in each segment of the models. Conversely, the latter type of models is characterised by smooth transitions and relatively more complex constitutive laws. In both the classes of models one can find rate-dependent or rate-independent models.

5.2.1.1 Piecewise-linear hysteretic models

Piecewise-linear hysteretic systems are capable to describe hysteretic behaviour by recurring to relatively simple equations through the assumption that the yield transitions are sharp and that the relationship between the restoring force and displacement is linear in each segment of the model. In this group fall elastoplastic, bilinear and polylinear hysteretic models.

The motion of an oscillator with nonlinear stiffness is described by Newton’s second law in the form:

$$m\ddot{x} + f(x, \dot{x}) = u(t) \quad (5.7)$$

where m represents the mass of the system, x the displacement, u the external force, f the internal restoring force of the system.

By defining k as the initial stiffness of a nonlinear hysteretic system with a post-yielding stiffness of αk , then the restoring force of the system may be expressed as:

$$f = \alpha kx + (1 - \alpha)kz \tag{5.8}$$

where x is, again, the displacement of the system and z is the normalised hysteretic force component that depends on the history of displacement.

Figure 5.6 shows an elastoplastic hysteretic oscillator, which can be idealised as a system composed by two elements: a linear spring element of stiffness k and a Coulomb slip element that slips when the force level reaches $k x_y$. This particular system can be considered as a subcase of equation (5.8) when α is set to be zero.

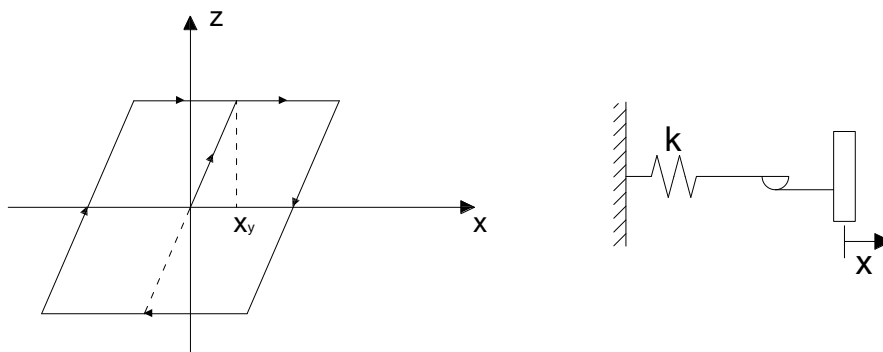


Figure 5.6 - (a) Elastoplastic model, restoring force and displacement phase plot (b) Idealised system.

Bilinear hysteretic models have been extensively studied and several examples of these types of models can be found in literature (see for instance [30,31,32,33,34,35,36]). Usually, in order to generalise the formulation of bilinear hysteretic models, the hysteretic force can be defined by its time derivative:

$$\dot{z} = \dot{x} \left[1 - H(\dot{x})H(z - x_y) - H(-\dot{x})H(-z - x_y) \right] \tag{5.9}$$

where $H(x)$ identifies the so-called Heaviside's unit step function, defined by:

$$H(x) = \begin{cases} 1 & \text{for } x \geq 0 \\ 0 & \text{for } x < 0 \end{cases} \tag{5.10}$$

This means that the relative velocity of the Coulomb slip element must be zero when $-x_y < z < x_y$ and equal to \dot{x} when either $z = x_y$ with $\dot{x} > 0$ or $z = -x_y$ with $\dot{x} < 0$.

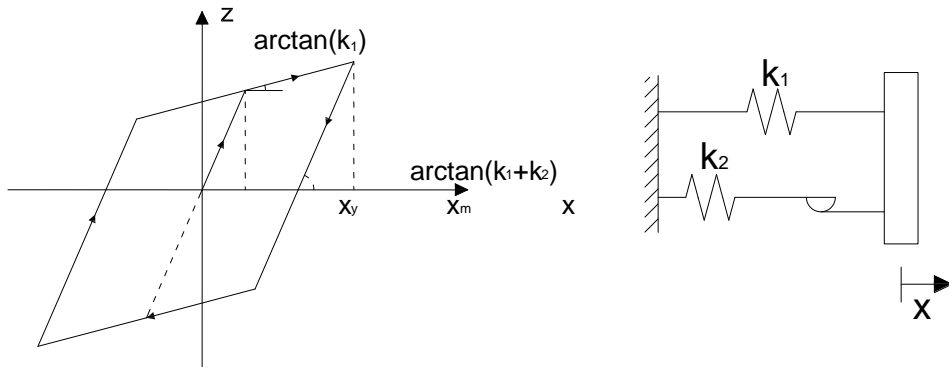


Figure 5.7 - (a) Bilinear model as studied by Iwan [32] (b) Idealised system.

Conceptually, this model behaves similarly to the elastoplastic model except for the introduction of a linear spring (see figure 5.7b). Actually, bilinear models can be considered as refinements of the elasto-plastic model. What is evident from both elastoplastic and bilinear model is that they are unable to adequately represent deterioration and the restoring force behaviour observed in the preceding section. In fact, even though the effective stiffness decreases monotonically with increasing the amplitude of the response, the system recovers its full initial stiffness.

The model proposed by Clough and Johnston in 1966 [37] was one of the first attempts to characterise the deteriorating properties of structural elements. The effective stiffness of the Clough-Johnston's model, when the amplitude of the response increases, corresponds to the stiffness of the elasto-plastic model (see figure 5.8). Anyway, unlike the elasto-plastic model, when the amplitude of response decreases, the effective stiffness recovers only slightly from its minimum value. The parameter which describes the decrease in effective stiffness is the product of the yield displacement and initial stiffness. Anyway, this model is not able to provide a detailed fit of the entire effective stiffness diagram and it has been observed in [38] that, even when the model produces a good fit of the effective stiffness diagram, it gives hysteresis loops whose shapes are quite different from experimental data.

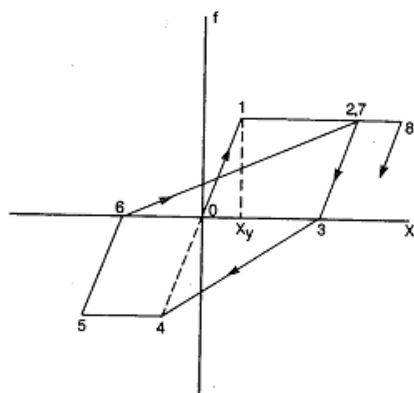


Figure 5.8 - The model proposed by Clough and Johnston [37].

A further evolution in the field of piecewise-linear models was the one proposed in 1970 by Takeda *et al* [39] for concrete elements. This model included stiffness changes at flexural cracking and yielding, and also strain-hardening characteristics. The unloading stiffness was reduced by an exponential function of the previous maximum deformation. Takeda *et al* also prepared a set of rules for load reversal within the outermost hysteresis loop, improving in this way the Clough-Johnston model. A piecewise linear backbone curve was defined by two break points at cracking and assumed to be symmetric with respect to the origin. The hysteresis rules were developed on the basis of experimental observation of reinforced concrete members under load reversal. In the end sixteen different rules were used to determine the stiffness of a frame member at each load level (see figure 5.9). In literature it is possible to find various proposal of modification to the Takeda's model, in order to simplify the set of rules, such the Takeda's modified model proposed by Otani [40] in 1974 or the so-called Q-Hyst model proposed by Saiidi and Sozen in [41] in 1979.

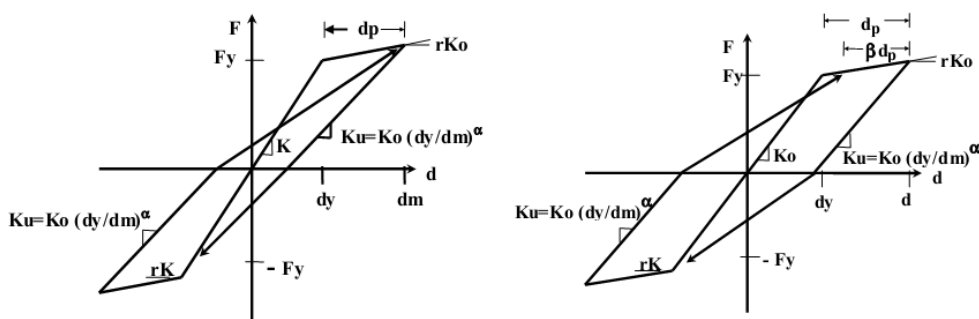


Figure 5.9 - Takeda's model [39].

Another approach which derives from the models illustrated in this section is the distributed-element model (or the so-called Iwan's model, firstly proposed in 1986). In this

case Iwan [42,43] assumed that a general hysteretic system may be thought as consisting of a large number of ideal elasto-plastic elements, each with the same elastic stiffness but having different yield levels. Iwan assumed a model consisting of three distinct types of physical elements arranged in the configuration shown in Figure 5.10. Accordingly to Iwan, one can distinguish in three main categories of elements:

- 1) linear elements: the combined stiffness of these elements is indicated with k_e ;
- 2) deteriorating elasto-plastic elements: the deteriorating elements are similar to elasto-plastic elements except that they “break” when their relative displacement exceeds a certain limit. These elements are composed by a linear spring indicated by k_i in series with a slip Coulomb dampers allowing for a maximum force equal to $k_i \cdot x_{y_i}$ where x_{y_i} is the yield displacement. If the relative displacement becomes larger than a value $\beta_i x_{y_i}$ the element break and its contribution to the restoring force becomes zero.
- 3) elasto-plastic element(s) may be considered as a subclass of the deteriorating elasto-plastic elements for which $\beta_i < x_{\max} / x_{y_i}$. In the classical formulation of the model there is one of these elements.

The deteriorating elements account for the loss of stiffness of the structure when the amplitude of oscillation increases. This observed phenomenon is usually continuous; therefore a high number of deteriorating elements is desirable. Anyway, the number of parameters of the model may result to be too big for great value of N , therefore some assumptions on the parameters may be done. Iwan suggested utilising a value of β equal for all the elements and to link k_i with x_{y_i} through the following equation:

$$k_i = \frac{\gamma}{x_{y_i}^2}; \quad i=1, \dots, N \quad (5.11)$$

where γ is a proportionally constant independent of i . Equation (5.11) specifies that each deteriorating element spring stores the same amount of elastic energy at yield. In this way, the number of parameters associated to the N deteriorating elements is reduced to $N+2$, instead of $3N$. Therefore, the force-deflection relation for the entire system may be generally written as:

$$f = \sum_{i=1}^n \frac{f_i}{N} + k_i \cdot x \frac{(N-n)}{N} \quad \dot{x} > 0 \quad (5.12)$$

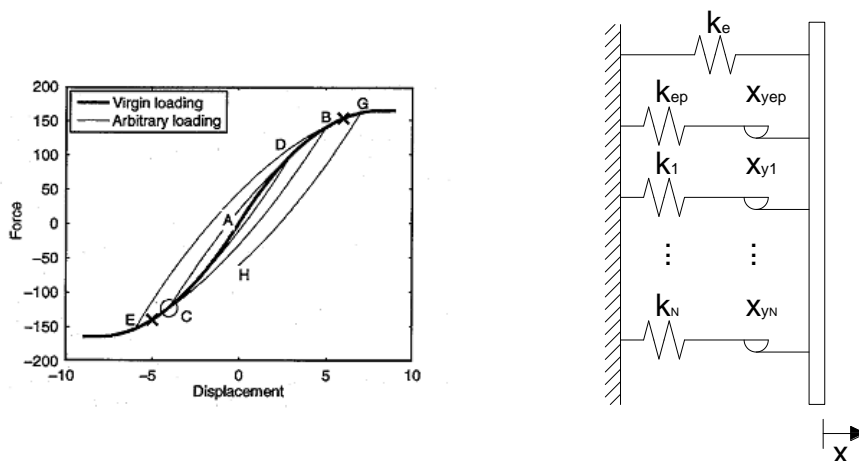


Figure 5.10 - (a) The deteriorating-distributed-element model, for high values of N is characterised by smooth transitions (b) Idealised system [42].

5.2.1.1.1 Masing model and its evolutions

One of the first models conceived for the idealisation of systems showing an hysteretic behaviour is the model proposed by Masing in 1926 [44]. This model assumed that a metal body consists of a collection of body elements each with the same elastic stiffness but different yield limits in a similar fashion as in the previously mentioned Iwan's model. Masing assumed that if the load-deflection curve of the entire system at the "virgin" loading is symmetric about the origin it may be given by the odd function $g(x, f) = 0$, where f is the restoring force corresponding to displacement x . Defining as x_0 and f_0 the coordinates for the reversal of the loading branch, one can define the geometric shape of the initial loading curve by stretching it of two in both direction:

$$g\left(\frac{f - f_0}{2}, \frac{x - x_0}{2}\right) = 0 \quad (5.13)$$

A peculiar characteristic of Masing's model is that under arbitrary transient loading it exhibits changes in strength without any physical reason. Iwan's model would fall under the Masing model class if it were not for this property [45]. Jayakumar [46] in 1987 proposed an extension of the Masing model entailing two rules:

- incomplete loops: the equation of any hysteretic response curve can be obtained by applying the original Masing rule to the virgin loading curve using the latest point of load reversal.
- complete loops: if an interior curve under continued loading or unloading crosses a curve described in a previous load cycle, the force deformation curve follows that of the previous cycle (Figure 5.11).

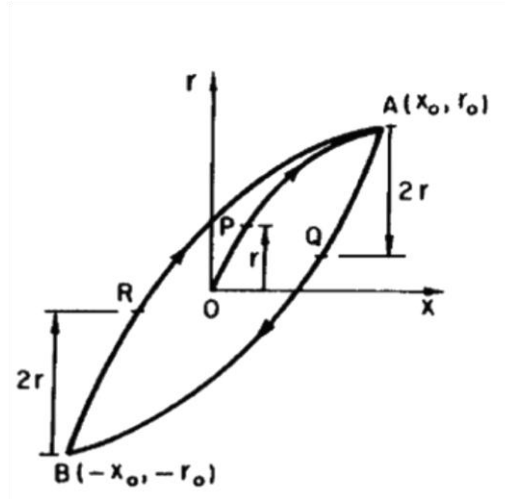


Figure 5.11 - Masing hysteresis loop

In the light of these two rules, a differential formulation of the model can be achieved:

$$\frac{df}{dx} = g\left(\frac{x-x^*}{2}, \frac{f-f^*}{2}\right) \quad (5.14)$$

where (x^*, f^*) are the coordinates of the point of load reversal chosen accordingly to the aforementioned rules. For what concerns the virgin loading, Jayakumar [46] proposed a relationship for the virgin loading of this type:

$$\frac{df}{dx} = k \left[1 - \left| \frac{f}{f_u} \right|^n \right] \quad (5.15)$$

and, for the successive loading branches, the force-deformation relation, has to be modified accordingly to equation (5.14):

$$\frac{df}{dx} = k \left[1 - \left| \frac{f-f^*}{2f_u} \right|^n \right] \quad (5.16)$$

In both equations, k , r_u and n are three model parameters which should provide sufficient flexibility to capture the essential features of hysteretic behaviour of most structural systems. In the case of this modified Masing model, the hysteretic behaviour shown by an Iwan's model can be completely described without the need of characterising the single elements [46].

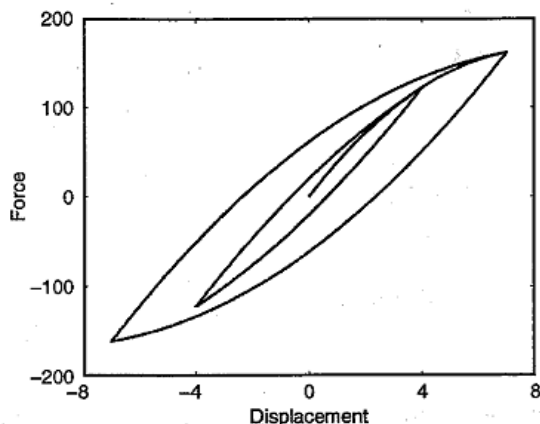


Figure 5.12 - Masing model hysteretic response for stable cyclic loading.

The simplicity of the Masing model allowed for its application in various fields, and several applications implemented different degrading laws in order to take into account the effects of deterioration. For instance, Vucetic [47] used the model to describe the behaviour of clay under irregular cyclic loading, using a deterioration index applied directly to the “virgin” curve. More sophisticated approaches were pursued by Thyagarajan [48] or Chiang [49] who used a distributed-element-model to generalise the Masing model able to describe deterioration allowing for partial loss of strength and stiffness in the single elements rather than complete breaking. Ashrafi and Smyth [45] recently proposed a set of rules for a Masing generalised model characterising deterioration by using a different set of distribution function.

5.2.1.1.2 *Ramberg-Osgood model*

The well-known formula proposed by Ramberg and Osgood [50], firstly proposed in 1943, describes stress-strain relations in terms of three parameters for monotonic loading starting from the origin. It was used by Jennings [51] to define a more general nonlinear hysteretic force-deflection relation. The “virgin” curve of this relation as defined by Jennings is clearly inspired by the Ramberg-Osgood formula:

$$\frac{x}{x_y} = \frac{f}{f_y} + \alpha \left(\frac{f}{f_y} \right)^n \tag{5.17}$$

Where x and f have their usual meaning, x_y is the yielding displacement, f_y is the yielding force, α is a positive constant and $n > 1$ is a positive odd (in order to assure symmetry about the origin) integer. It is worth noticing that a linear structure is characterized by $\alpha=0$ when an elasto-plastic structure is approached as n tends to ∞ (with α greater than 0). By using the concept already exposed for the Masing model, Jennings modified equation (5.17) to formulate a hysteretic law as follows:

$$\frac{x - x_i}{2x_y} = \frac{f - f_i}{2f_y} + \alpha \left(\frac{f - f_i}{2f_y} \right)^n \quad (5.18)$$

where $(x_i / x_y, f_i / f_y)$ is the most recent point at which the direction of the loading has been reversed (see figure 5.13). For what concerns earthquake excitation Jennings defined two additional properties which specifies in which way the branch curves are linked together to represent arbitrary loading patterns. In his approach, force-deflection values are given by the hysteresis curve originating from the point of most recent loading reversal until the upper or lower boundary is contacted. Thereafter the force-deflection values are given by that boundary until the direction of loading is again reversed.

Matzen and McNiven [52] in 1976 tested a single story steel frame structure on a shaking table and inferred that Ramberg-Osgood model do not match the real hysteretic loops for the entire duration of the test. They concluded that two sets of Ramberg-Osgood parameters are required to predict the response of time-histories and hysteretic loops in a better way: one set has to be used in the brief initial phase during which the structure responds approximately elasto-plastically and another set must be used when the hysteretic behaviour has stabilized.

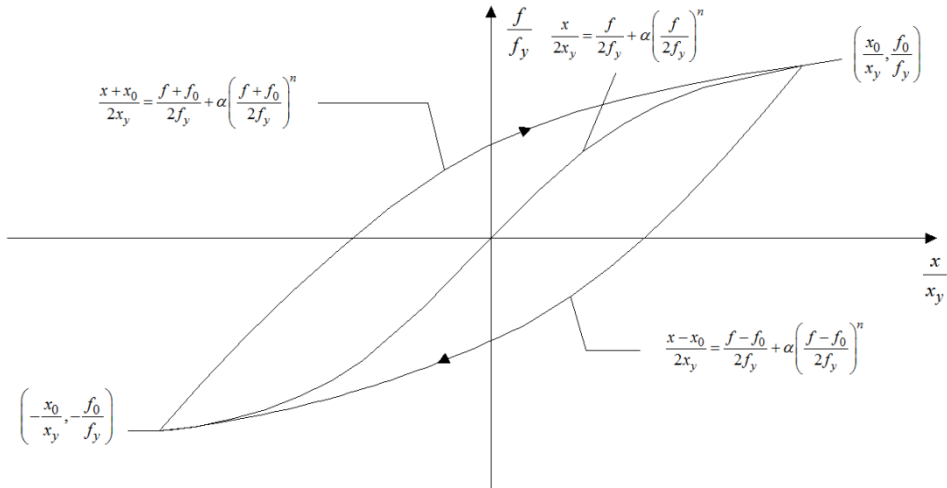


Figure 5.13 - Typical hysteretic loop of a Jennings' model governed by a Ramberg-Osgood law.

5.2.1.1.3 Bouc-Wen models

The model proposed by Bouc in [53] in 1971 is one of the most successful models in the field of hysteretic models as it is witnessed by the several modifications that have been proposed in literature to the original model. The most important contribution to the original model is probably the one given by Wen in [54] 1976, so important, that nowadays the model is known as “Bouc-Wen” model. The model proposed by Bouc-Wen is to

construct a hysteretic restoring force which satisfies the following first-order nonlinear differential equation:

$$\begin{cases} m\ddot{x} + c\dot{x} + f = u \\ \dot{f} = A \cdot \dot{x} - \beta \cdot \dot{x} \cdot |f|^n - \gamma |\dot{x}| \cdot f \cdot |f|^{n-1} \end{cases} \quad (5.19)$$

where A , β , γ and n are model parameters. In equation (5.19) the parameter A is the linear stiffness of the oscillator, $\beta > 0$, $\gamma \in [-\beta, \beta]$ and $n > 0$ are constants affecting the form of the hysteresis loops. The exponent n is the parameter introduced by Wen: when it is large enough, force-displacement curves are similar to those of an elastic-perfectly-plastic model, instead, when is equal to 1 the model collapses in the original Bouc model (see figure 5.14).

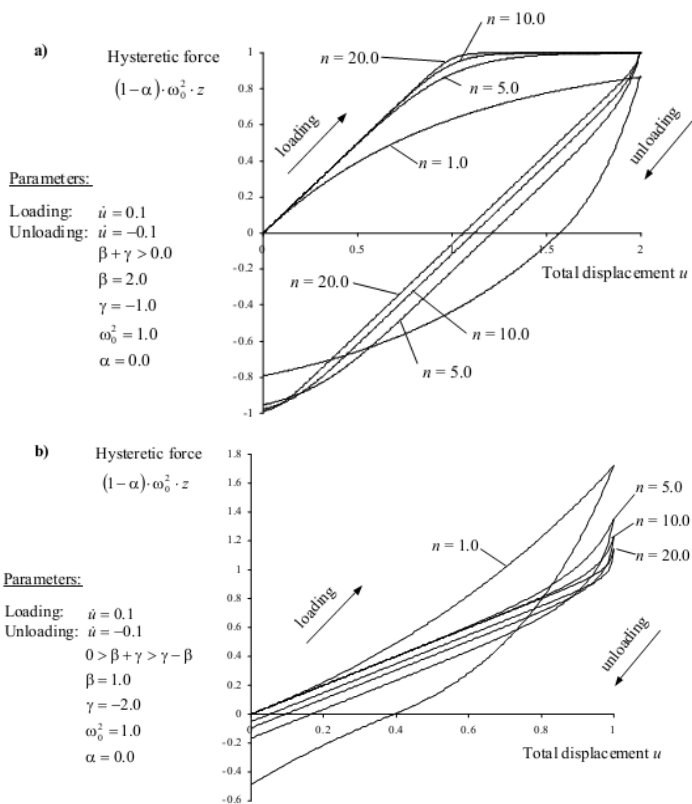


Figure 5.14 – a) Hysteretic force vs total displacement, effects of increasing n on softening hysteresis. b) Similar to a) but the effects of increasing n are on hardening hysteresis [55].

Adjusting the values of the model parameters, one can construct a large class of hysteretic systems, such as hardening or softening, and narrow- or wide-band systems. Baber listed

a series of relationships between β and γ and their effect on the hysteresis, reported in table 5.1 [56].

$\beta + \gamma > 0$ $\gamma - \beta < 0$	Weak softening
$\beta + \gamma > 0$ $\gamma - \beta = 0$	Weak softening on loading, mostly linear unloading
$\beta + \gamma > \beta - \gamma$ $\beta - \gamma < 0$	Strong softening loading and unloading, narrow hysteresis
$\beta + \gamma = 0$ $\gamma - \beta < 0$	Weak hardening
$0 > \beta + \gamma$ $\beta + \gamma > \gamma - \beta$	Strong hardening

Table 5.1 - Relationship between β and γ and their effects on the hysteresis.

Despite its simplicity and the fact that it fulfils the 2nd principle of thermodynamics, the Bouc-Wen model is affected by the so-called “violation of the Drucker-Prager postulate”. A comprehensive discussion of these topics is presented in [57,58] and [59].

Successively, in 1981 Baber and Wen [60] proposed a differential equation model allowing for both stiffness and strength degradation, allowing several problems in civil engineering to be studied, such as damage evaluation of buildings, soil-structure interaction and liquefaction of soil deposits. The formulation introduced other parameters with respect to the original Bouc-Wen model:

$$\begin{cases} m\ddot{x} + c\dot{x} + \alpha K_0 x + f = u \\ \dot{f} = \frac{(1-\alpha)}{\eta} \left[A - \nu |f|^n (\gamma + \beta \operatorname{sgn}(f \cdot \dot{x})) \right] \dot{x} \end{cases} \quad (5.20)$$

where α and K_0 were already introduced in a previous paper by Wen [61], and they define respectively the post to pre-yielding stiffness ratio and the initial total stiffness. One can observe that the simultaneous presence of the parameter K_0 and A is redundant (this problem was not noticed in the original paper. For what concerns strength degradation it is completely ruled by the parameter ν , while the stiffness degradation is ruled by the parameter η . The authors proposed three energy-dependent evolution laws for the parameters A , ν and η :

$$\begin{cases} A(e) = A_0 - \delta_A \cdot e \\ \nu(e) = \nu_0 - \delta_\nu \cdot e \\ \eta(e) = \eta_0 - \delta_\eta \cdot e \end{cases} \quad (5.21)$$

where A_0 , ν_0 and η_0 are the initial values of the degradation functions while e is a generally increasing function, usually chosen to be the total dissipated energy.

A further modification to the Bouc-Wen model was proposed by Baber and Noori [62] in the attempt to introduce in the model the possibility to represent also pinching effects in the so-called Bouc-Wen-Baber-Noori model (1985). These authors chose to introduce a pinching spring in the original model, in series with the hysteretic element corresponding to the force f . Other three parameters that define the pinching function have been added to the aforementioned ones:

$$\begin{cases} m\ddot{x} + c\dot{x} + \alpha K_0 x + f = u \\ \dot{f} = \frac{K_h K_p}{K_h + K_p} \dot{x} \\ K_h = \frac{(1-\alpha)}{\eta} \left[A - \nu |f|^n (\gamma + \beta \operatorname{sgn}(f \cdot \dot{x})) \right] \\ K_p = \left(\frac{1}{\sqrt{2\pi} Z_\sigma} \Delta x \cdot e^{-\frac{z^2}{2Z_\sigma^2}} \right)^{-1} \end{cases} \quad (5.22)$$

The degradation rules are those defined by equation (5.21), still depending on energy e . The same authors proposed a different way to model pinching effects by using a pinching inducing function which multiplies the non pinching hysteretic stiffness K as defined by the following set of differential equations:

$$\begin{cases} m\ddot{x} + c\dot{x} + \alpha K_0 x + f = u \\ \dot{f} = K\dot{x} \\ K = (1-\alpha) \frac{h}{\eta} \left[A - \nu |f|^n (\gamma + \beta \operatorname{sgn}(f \cdot \dot{x})) \right] \end{cases} \quad (5.23)$$

with

$$\left\{ \begin{array}{l} h(f, e) = 1 - \zeta_1 \exp\left(-\frac{f^2}{2\zeta_2^2}\right) \\ \zeta_1(e) = \zeta_{1,0} (1 - \exp(-p \cdot e)) \\ \zeta_2(e) = (\zeta_0 + \delta_\xi)(\lambda + \zeta_1(e)) \end{array} \right. \quad (5.24)$$

where $\zeta_{1,0}$, ζ_0 , δ_ξ , λ and p are pinching parameters. In this second model the mechanical interpretation of pinching as two spring in series is lost, but the versatility of the model is improved. In fact, the dependency of h from the variable f is of Gaussian type allows for good mathematical tractability of the model.

In 1995, Foliente [63] proposed a further modification of the Bouc-Wen model aimed at improving the pinching modelling. He adopted a function h with a non-zero mean \bar{f} . Foliente's model is still defined by equations (5.23) and (5.24) with the following proposed modification for the pinching function h :

$$\left\{ \begin{array}{l} h(f, \text{sgn}(\dot{x}), e) = 1 - \zeta_1 \exp\left(-\frac{(f - \bar{f} \text{sgn}(\dot{x}))^2}{\zeta_2^2}\right) \\ \bar{f}(e) = q \left(\frac{1}{v(\gamma + \beta)}\right)^{\frac{1}{n}} \end{array} \right. \quad (5.25)$$

where q is a parameter governing strength degradation. This modification allows for a better fitting of experimental data. Moreover, Foliente noticed the redundancy of the parameters K_0 and A and proposed to solve the problem by setting $A=1$.

Recently, in 2000, Sivaselvan and Reinhorn [64] proposed another modification of the Bouc-Wen model, in order to have parameters with a clear physical meaning. In this model the viscous part of the restoring force is not considered and the pinching effect is introduced again by a pinching spring in series with the hysteretic element. The model is defined by the following set of differential equations:

$$\left\{ \begin{array}{l}
 m\ddot{x} + \alpha K_0 x + f = u \\
 \dot{f} = \frac{K_h K_p}{K_h + K_p} \dot{x} \\
 \dot{e}_d = \begin{cases} f\dot{x} - \frac{f \cdot \dot{f}}{2 \cdot R_k \cdot K_0} & f\dot{x} \geq 0 \\ 0 & f\dot{x} < 0 \end{cases} \\
 K_h = (R_k - \alpha) K_0 \left[1 - \left| \frac{f}{f_y} \right|^n (\eta_1 \operatorname{sgn}(f \cdot \dot{x}) + \eta_2) \right] \\
 K_p = \left\{ \sqrt{\frac{2}{\pi}} \frac{s}{f_\sigma^*} \exp \left[-\frac{1}{2} \left(\frac{f^* - \bar{f} \operatorname{sgn}(\dot{x})}{f_\sigma^*} \right)^2 \right] \right\}^{-1} \\
 x_{\max}^+(t) = \max_{\tau \leq t} (x(\tau)) \\
 x_{\max}^-(t) = \min_{\tau \leq t} (x(\tau))
 \end{array} \right. \quad (5.26)$$

It is worth noticing that the stiffness degradation parameter R_k has the same meaning as the parameter η in the previous version of the model and the same holds for the strength degradation parameter R_z and ν . The authors suggested in the original paper a series of possible degradation rules for R_k and R_z and to adopt a pivot degradation rule and a strength degradation rule depending on the dissipated energy e_d and on the maximum positive and negative displacement attained during the applied history. For what concerns the degrading and pinching functions, Sivaselvan and Reinhorn [64] proposed to use the following ones:

$$\left\{ \begin{array}{l}
 f_y = f_{y,0} \cdot R_z \\
 R_f = \left[1 - \frac{|u_{\max}^{+/-}|}{|u_{ult}^{+/-}|} \frac{1}{\beta_1} \right] \left(1 - \frac{\beta_2}{1 - \beta_2} \frac{e_d}{e_{d,ult}} \right) \\
 R_k = \frac{f + \delta \cdot f_y}{K_0 \cdot x + \delta \cdot f_y} \\
 f_\sigma = \sigma f_y \\
 \bar{f} = \lambda f_y \\
 \Delta x_p = R_s (u_{\max}^+ - u_{\max}^-)
 \end{array} \right. \quad (5.27)$$

where σ , λ and R_s are pinching parameters.

5.2.1.1.4 A modified Bouc-Wen model

Li *et al* [65] and Ceravolo *et al* in [66,67] proposed a modified Bouc-Wen model allowing for both stiffness degradation and slip applicable also to MDOF systems. Ceravolo *et al* [66,67], in order to account for slip in equation (5.19), an inverse sigmoid function is introduced [66]:

$$x_s(f) = s \frac{(1 - e^{-\mu_s \cdot f})}{(1 + e^{-\mu_s \cdot f})}, \quad (5.28)$$

where f defines a spring force, s the amount of slip and μ_s a coefficient that controls the inverse of the tangent near the origin. This function is depicted in where, in agreement with [65,68], s precisely defines only half of the total slip. In greater detail, this slip model is expected to capture several phenomena in a steel-concrete composite structure, like detachments at steel-concrete interfaces, bolt clearances, clearances at beam-to-column joints, clearances at column bases, etc.

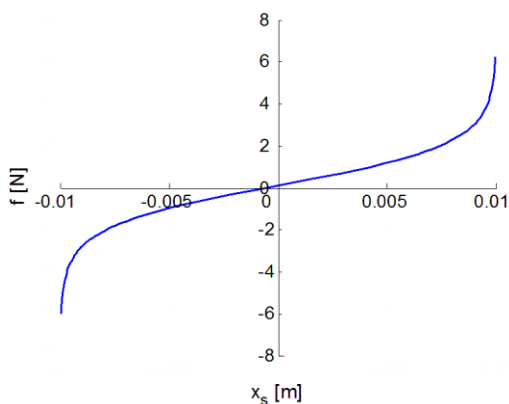


Figure 5.15 - A slip function.

The slip spring governed by (5.28) is assumed to operate in series with a Bouc-Wen hysteretic spring, *i.e.*

$$x = x_s + x_{BW} \tag{5.29}$$

This assumption is illustrated in figure 5.16.

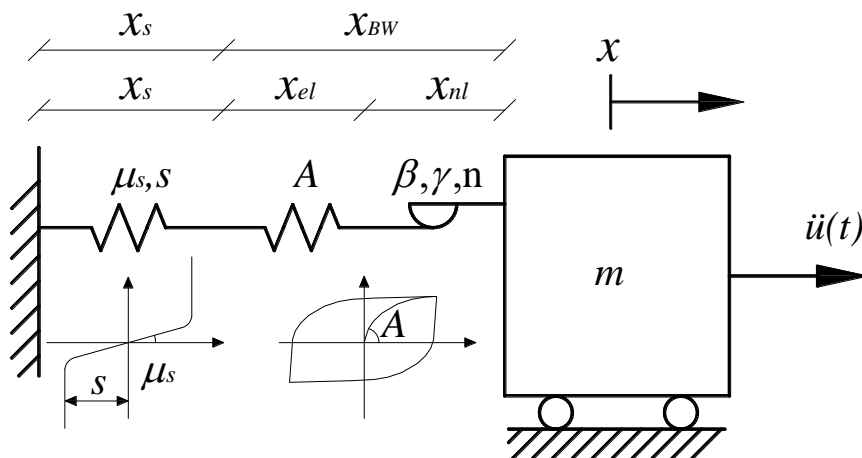


Figure 5.16. Slip and Bouc-Wen springs in series for a SDOF system.

From equation (5.28) one can define the inverse of the tangent stiffness $k_s(f)$ associated with slip, *i.e.*

$$\frac{1}{k_s(f)} = \frac{dx_s(f)}{df} = \frac{2\mu_s s}{(1 + e^{\mu_s f})^2} e^{\mu_s f} > 0 \tag{5.30}$$

Similarly, the tangent stiffness of the Bouc-Wen model is obtained from (5.19) by derivation with respect to x_{BW} , i.e.

$$k_{BW}(f, \text{sign}(\dot{x}_{BW} \cdot f)) = A - (\beta \cdot \text{sign}(\dot{x}_{BW} \cdot f) + \gamma) |f|^n \quad (5.31)$$

Since $A > 0$ and $k_{BW}(f, \text{sign}(\dot{x} \cdot f)) > 0$ for all given f and \dot{x} , then $\text{sign}(\dot{x}) = \text{sign}(\dot{x}_{BW}) = \text{sign}(\dot{x}_s)$. In other words, an increase of f entails an increase of x_{BW} , x_s and, due to (5.29), of x . Thus, the stiffness formulation of the Bouc-Wen model reads:

$$\dot{f} = k_s(f) \cdot \dot{x}_s = k_{BW}(f, \text{sign}(\dot{x} \cdot f)) \cdot \dot{x}_{BW} \quad (5.32)$$

and the equivalent stiffness of the springs in series, \tilde{k} , becomes:

$$\tilde{k}(f, \text{sign}(\dot{x} \cdot f)) = \frac{k_s(f) k_{BW}(f, \text{sign}(\dot{x} \cdot f))}{k_s(f) + k_{BW}(f, \text{sign}(\dot{x} \cdot f))} = \left(\frac{2\mu_s s}{(1 + e^{\mu_s f})^2} e^{\mu_s f} + \frac{1}{A - (\beta \text{sign}(\dot{x} \cdot f) + \gamma) |f|^n} \right)^{-1} \quad (5.33)$$

To sum up, the differential system for a SDoF model endowed with the Bouc-Wen hysteretic law in series with a slip component, takes following form

$$\begin{cases} m\ddot{x} + f = -m\ddot{u} \\ \dot{f} = \tilde{k}(f, \text{sign}(\dot{x} \cdot f)) \cdot \dot{x} \end{cases} \quad (5.34)$$

If we define \bar{k} as the equivalent stiffness that we would obtain by excluding hysteresis from equation (5.33), it can be proven that system (5.34) is equivalent to

$$\begin{cases} m\ddot{x} + f = -m\ddot{u} \\ \dot{f} = \bar{k}(f)(\dot{x} - \dot{x}_{nl}) \\ \dot{x}_{nl} = \frac{1}{A} \beta_p(f, \text{sgn}(\dot{x})) \dot{x}_{BW} \\ \frac{1}{\bar{k}(f)} = \frac{1}{A} + \frac{1}{k_s(f)} \end{cases} \quad (5.35)$$

with

$$\beta_p(f, \text{sgn}(\dot{x})) = (\beta \text{sgn}(\dot{x}f) + \gamma) |f|^n \quad (5.36)$$

and

$$\dot{x}_{BW} = \dot{x} - \dot{x}_s = \dot{x} - \frac{\dot{f}}{k_s(f)}. \quad (5.37)$$

This formulation based on a model with slip and hysteresis is easier to generalise to the 2-DoF case than equation (5.34).

5.2.1.1.5 Model for a 2-DOF system

In this subsection, the modified Bouc-Wen model will be extended to chain-like 2-DoF systems. With reference to a 2-DoF system and in accordance with equation (5.29), one can express the global displacements in terms of flexibility, by summing both linear and nonlinear components. First, we introduce the nonlinearity caused by slip, assuming that nonlinear restoring forces may be combined according to a chain-like system, i.e.,

$$\begin{Bmatrix} x_1 \\ x_2 \end{Bmatrix} = \begin{bmatrix} k_{11} & k_{12} \\ k_{12} & k_{22} \end{bmatrix}_{el}^{-1} \begin{Bmatrix} f_1 \\ f_2 \end{Bmatrix} + \begin{Bmatrix} x_{s,1}(f_1 + f_2) \\ x_{s,2}(f_2) + x_{s,1}(f_1 + f_2) \end{Bmatrix} \quad (5.38)$$

where

$$\begin{bmatrix} K_{el} \end{bmatrix} = \begin{bmatrix} k_{11} & k_{12} \\ k_{12} & k_{22} \end{bmatrix}_{el} \quad (5.39)$$

represents the condensed stiffness matrix of the underlying linear system, which will be time variant during the identification process; $x_{s,1}$ and $x_{s,2}$ define the nonlinear inter-storey drifts at the lower and upper storey, respectively. These displacements are assumed to depend on the forces $f_1 + f_2$ and f_2 , respectively, according to a shear-type behaviour.

Equation (5.35) may be expressed in an explicit form, in accordance with equation (5.28)(7), and differentiated with respect to time:

$$\begin{Bmatrix} \dot{x}_1 \\ \dot{x}_2 \end{Bmatrix} = \begin{bmatrix} k_{11} & k_{12} \\ k_{12} & k_{22} \end{bmatrix}_{el}^{-1} \cdot \begin{Bmatrix} \dot{f}_1 \\ \dot{f}_2 \end{Bmatrix} + \begin{bmatrix} \frac{2e^{\mu_{s,1}(f_1+f_2)}\mu_{s,1}s_1}{(1+e^{\mu_{s,1}(f_1+f_2)})^2} & \frac{2e^{\mu_{s,1}(f_1+f_2)}\mu_{s,1}s_1}{(1+e^{\mu_{s,1}(f_1+f_2)})^2} \\ \frac{2e^{\mu_{s,1}(f_1+f_2)}\mu_{s,1}s_1}{(1+e^{\mu_{s,1}(f_1+f_2)})^2} & \frac{2e^{\mu_{s,2}f_2}\mu_{s,2}s_2}{(1+e^{\mu_{s,2}f_2})^2} + \frac{2e^{\mu_{s,1}(f_1+f_2)}\mu_{s,1}s_1}{(1+e^{\mu_{s,1}(f_1+f_2)})^2} \end{bmatrix} \begin{Bmatrix} \dot{f}_1 \\ \dot{f}_2 \end{Bmatrix} \quad (5.40)$$

The second part of (5.40) clearly assumes the form of the product of a nonlinear flexibility matrix, $[K_s]^{-1}$, due to slip contribution, with the time-derivative of a force vector $\{f\} = (f_1, f_2)^T$. Therefore by inversion, we can define $[\bar{K}(f)]$ that extends to a 2-DoF system, the stiffness operator $\bar{k}(f)$ introduced in Eq. (5.35). Therefore, the equations of motion associated with the frame system assume the following form:

$$\begin{cases} [M] \cdot \{\ddot{x}\} + \{f\} = -[M] \cdot \{\ddot{u}_g\} \\ \{\dot{f}\} = [\bar{K}(f)] \cdot \{\dot{x}\} \\ [\bar{K}(f)]^{-1} = [K_{el}]^{-1} + [K_s(f)]^{-1} \end{cases} \quad (5.41)$$

In order to take into account hysteresis, a Bouc-Wen model is assumed to be in series with both the slip and the linear spring, as shown in figure 5.16 for a SDoF system. Therefore the system (5.41) is modified as follows:

$$\begin{cases} [M] \cdot \{\ddot{x}\} + \{f\} = -[M] \cdot \{\ddot{u}_g\} \\ \{\dot{f}\} = [\bar{K}(f)] (\{\dot{x}\} - \{\dot{x}_{nl}\}) \\ \{\dot{x}_{nl}\} = [K_{el}]^{-1} [\beta^p] \cdot \{\dot{x}_{BW}\} \\ [\bar{K}(f)]^{-1} = [K_{el}]^{-1} + [K_s(f)]^{-1}, \end{cases} \quad (5.42)$$

where $\{\dot{x}_{BW}\} = \{\dot{x}\} - \{\dot{x}_s\} = \{\dot{x}\} - [K_s(f)]^{-1} \{\dot{f}\}$. The matrix $[\beta^p]$ defines the hysteretic part of the restoring force vector $\{f\}$,

$$\begin{aligned} \left[\beta^p \right] &= \beta_p \left(f_1, f_2, \dot{x}_{BW,1}, \dot{x}_{BW,2}; \beta_1, \gamma_1, n_1, \beta_2, \gamma_2, n_2 \right) = \\ &\left[\begin{array}{cc} \dot{f}_p \left(f_1 + f_2, \dot{x}_{BW,1}; \beta_1, \gamma_1, n_1 \right) + \dot{f}_p \left(f_2, \dot{x}_{BW,2} - \dot{x}_{BW,1}; \beta_2, \gamma_2, n_2 \right) & -\dot{f}_p \left(f_2, \dot{x}_{BW,2} - \dot{x}_{BW,1}; \beta_2, \gamma_2, n_2 \right) \\ -\dot{f}_p \left(f_2, \dot{x}_{BW,2} - \dot{x}_{BW,1}; \beta_2, \gamma_2, n_2 \right) & \dot{f}_p \left(f_2, \dot{x}_{BW,2} - \dot{x}_{BW,1}; \beta_2, \gamma_2, n_2 \right) \end{array} \right] \end{aligned} \quad (5.43)$$

supposing a chain-like hysteretic nonlinearity, and \dot{f}_p denotes a Bouc-Wen type of hysteresis:

$$\dot{f}_p \left(f, \dot{x}_{BW}; \beta, \gamma, n \right) = |f|^n \left[\beta \operatorname{sign}(f \dot{x}_{BW}) + \gamma \right] \quad (5.44)$$

It is assumed $\beta_i > 0$, $\gamma_i \in [-\beta_i, \beta_i]$ and $n_i > 0$ in equation (5.44), thus, a softening behaviour is simulated. Additional information about Bouc-Wen model properties can be found in [69, 70, 71].

5.2.1.1.6 Endochronic models

Endochronic theory was originated by Valanis [72] as a description of the mechanical behaviour of metals, such as strain hardening, unloading and reloading, cross-hardening, continued cyclic strainings and sensitivity to strain rate. Using Valanis' concepts, Bazant extended the theory in order to describe the behaviour of a wide range of materials, such as rock, sand, concrete, reinforced concrete under various conditions. For instance, liquefaction of sand and inelasticity and failure of concrete were described. This theory appears to have the capability of characterizing a broad range of inelastic behaviours and loading conditions without recourse to additional yield conditions and hardening rules.

A simple endochronic model for uniaxial behaviour of metals is given by the following relation:

$$d\varepsilon = \frac{1}{E} d\sigma + \frac{\sigma}{ZE} |d\varepsilon| \quad (5.45)$$

where E is the elastic modulus and ZE is the limit stress of the material. This model is rate-independent and exhibits stress-strain behaviour as it is shown in figure 5.17. The paper by [73] shows that this behaviour violates Drucker's stability postulate and Ilyushin's postulate. Although the postulates of Drucker and Ilyushin are not strict physical or thermodynamic requirements for the behaviour of real materials, they do play an important role in the construction of rational theories or models of material behaviour for use in general dynamic problems. Through the construction of some simple examples, he showed that endochronic models are unsuitable for numerical solution of dynamical problems, for reasons such as non-unique solutions for a physical problem with unique solution, and small errors in initial and boundary conditions lead to a rapid deterioration of the accuracy of successive computations.

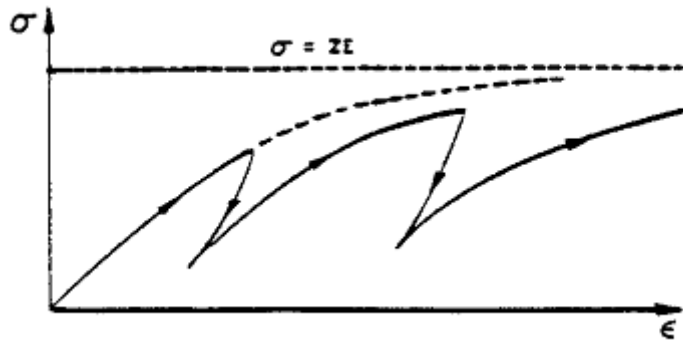


Figure 5.17 - Stress-strain relation for a simple endochronic model [73].

5.3 Nonlinear models for multiple degrees of freedom systems: recent theories and extensions

In the last twenty years, the extension of the normal modes of vibration of the linear vibration theory to mechanical systems that have nonlinear terms in the restoring forces has become a challenge for many authors. This has led to the so-called nonlinear normal modes (NNMs), which have great potential for applications in non-vibrating systems analysis, especially for building reduced-order models of nonlinear systems [74]. In [75], the authors developed a nonlinear component mode synthesis procedure by using the fixed-interface NNMs instead of the fixed-interface linear normal modes used in the traditional Craig-Bampton method.

The concept of nonlinear modes was first introduced by Rosenberg for studying conservative nonlinear systems with smoothly nonlinear restoring forces [76]. A NNM of an undamped discrete or continuous mechanical system can be defined as a synchronous periodic motion (PM) in which all the material points in the system reach their extrema and cross zero together. A PM for conservative systems is a closed trajectory in the phase space. For discrete conservative systems, a modal line represents the synchronous maximum oscillation of the system in the configuration space during an NNM motion. Linear systems possess straight modal lines, but in nonlinear systems, the modal lines can be either straight or curved.

Rosenberg classified the straight modal curves as similar NNMs while all the other modal curves are called non-similar NNMs. Based on the previous definition for NNMs, Lyapounov [77] proved the existence of n synchronous PMs or NNMs in the neighbourhood of stable equilibrium points of n Degrees of Freedom (DoFs) Hamiltonian systems without internal resonance, *i.e.* with linearized eigenfrequencies not integrally related. Other authors [78] extended Lyapunov's result to systems with internal resonances. More precisely, Rosenberg [76] defined NNMs of a discrete system with n DoFs by the four following conditions: (1) the motions of every mass are equi-periodic $u_i(t) = u_i(t+T)$ for $i \in [1, n]$ and T being the period, (2) during any time interval of a half period, the system passes exactly once through its equilibrium, (3) during every time

interval of a half period, the velocities of all masses vanish at exactly one time and (4) when r is any one of the coordinates, in an NNM during any time interval of a half period, every u_i , can be written in the form $u_i = u_i(u_r)$, and can be single valued. These conditions are very restrictive on the motion of the system and, in general, mechanical systems need to satisfy special symmetry conditions to have NNMs following the criteria provided by Rosenberg. Following Rosenberg's pioneer work, several authors have developed methods for the computation of NNMs for discrete conservative systems with few DoFs (usually limited to 2 DoFs), such as various perturbation techniques [79], the method of multiple scales [80], which ensures that NNMs approach linear normal modes asymptotically as the nonlinearity disappears, the harmonic balance method [81], or the normal form theory [82].

Free oscillations of a non-conservative system are no longer synchronous and non-trivial phase differences are expected between the positional variables. Thus, to study NNMs in non-conservative systems, Shaw and Pierre [83,84] reformulated the definition of NNMs, introducing the concept of invariant manifolds based on the mathematical concept of an invariant of the phase space and on the center manifold theorem [85]. This approach will henceforth be referred to as the Invariant Manifold Approach (IMA) and, contrary to Rosenberg's approach, it does not imply the existence of a first integral of movement. The definition of an NNM invariant manifold is then given: "A *NNM invariant manifold* is a two-dimensional invariant manifold in the system's phase space that is tangent to the corresponding linear modal eigenspace at the stable equilibrium point. On this manifold, the system's dynamics is governed by an equation of motion involving a pair of state variables (a modal displacement-velocity). It behaves like a single-DoF system". The parametrisation of the invariant manifolds of the NNMs is then performed by using two independent reference variables; namely, a reference positional displacement and a reference positional velocity. In order to provide consistency with the linear terminology, Slater and Inman proposed six definitions for NNMs [86] using IMA. The first constructive technique for generating such manifolds (in the sense of IMA) used asymptotic methods to generate polynomials that approximate the manifold locally.

Nayfeh *et al.* [87] reformulated the IMA in a complex framework (complex invariant manifold formulation) which allows the calculation of higher-dimensional invariant manifolds for NNMs in systems with internal resonances [88]. Moreover, Pesheck *et al* [89] generalized the single mode (individually) NNM invariant manifold of dimension 2 to invariant multi-mode manifolds of dimension $2m$ where m is the number $m \geq 1$ of nonlinear modes taken into account in the method. The computational procedure used for the multi-mode invariant manifold approach proposed by these authors is similar to that previously given for an individually invariant manifold (see [84]) Approximations for weakly nonlinear systems can be easily built.

Many of the above mentioned methods for computing NNMs are based on perturbation expansions with a truncation of the series after the first leading order terms. They have the advantage of providing analytical expressions of the NNMs but they are often limited to weak nonlinearities or small amplitudes. In fact, due to the nature of the polynomial's approximation, divergence between the asymptotic approximation and the actual manifold may appear even at small amplitudes that can be slightly beyond the domain of linear validity. To remedy these limitations, Pesheck *et al* [90] defined an alternative set of co-ordinates for the IMA: the pair of modal amplitude-phase using the Van der Pol transformation. They proposed a series approximation over a chosen domain

instead of a local polynomial approximation. The nonlinear equations in the expansion coefficients were then deduced from a Galerkin projection and solved to achieve an approximation of the invariant manifold by minimising the error for the selected basis functions. Based on this new constructive technique for generating such manifolds, many applications have been used for a wide class of discrete or continuous systems. For example: with smooth or non-smooth restoring forces [91], with internal resonances [92], with non-proportional damping forces [93], or subjected to shocks or harmonic excitations [94].

Recently, a new formulation for the existence and computation of a NNM has been introduced by Bellizzi and Bouc [95] for the cases of both undamped and damped nonlinear systems [96]. In this approach, which we will call the modal representation approach (MRA), the NNM is constructed in terms of amplitude-phase, similarly to the previously mentioned approach of Pesheck *et al* [90]; however, the mode phase and frequency are here dependent on the amplitude and on the total phase.

Finally, it is worth mentioning two of the most popular methods for computing PMs: the so-called harmonic balance method (HBM) and the shooting method (SM). In contrast to the SM, the HBM is essentially a frequency-domain method where the PMs are derived from a truncated Fourier series. This technique, commonly used by engineers [97], can be considered as a particular case of the Ritz-Galerkin technique (see [81] for details). The principle of HBM has been used successfully for numerous applications even in the case of almost-periodic solutions when no rigorous mathematical foundation exists. SM is a numerical method for solving a boundary value problem by reducing it to the solution of an initial value problem (see [98] section 7.3). Here, it consists of finding a suitable initial condition, which induces a closed trajectory in the phase space. This leads to a boundary value problem where the boundary condition is, in fact, a periodicity condition.

An interesting feature of NNMs is that they must interact; unless initial conditions for a pure mode are specified. These interactions can become strong and even predominant for the overall dynamics, leading to instabilities and bifurcations of NNMs. So, either when the amplitude of a NNM becomes “too large” or when a bifurcation occurs, the techniques IMA [84] or MRA [95], fail when applied alone and the determination of a valid solution is not certain.

Their validity domain, *i.e.* the variation domain of the amplitude of the solution, is not known a priori. Therefore, the understanding of the NNMs, in association with their bifurcations, becomes very helpful to understand the dynamics of a nonlinear system. Thus, several authors are now searching to explore the NNMs at large amplitude of vibration, and, when possible, to detect all kinds of bifurcations along a NNM. The techniques previously cited for constructing NNMs generally lead to a set of nonlinear algebraic equations. At critical points, the Jacobian matrix associated with these nonlinear equations is singular or rank deficient. These equations generally depend on a varying free parameter called the control parameter which can be the period for PMs, the response frequency for free oscillations of conservative systems, or the excitation frequency for steady-state vibrations. In this case, continuation techniques [99,100] can be used to solve the equations by finding the continuation of a nonlinear solution with respect to the control parameter. These techniques are frequently encountered in parametric studies of nonlinear systems; they include the classical Newton-Raphson technique, arc-length and pseudo arc-length continuation methods, the asymptotic

numerical method, and so on. As the number of unknowns is increased by one, a new scalar equation must be added such that the corresponding Jacobian matrix has full rank. This way, critical points can be detected and all branches of solutions at these points can be calculated. The asymptotic numerical method [101] is a path-following technique based on high order power series expansions (via a perturbation method). In the pseudo arc-length continuation, the new scalar equation is that of an hyperplane which is perpendicular to the tangent at the operating point of the response curve at a determined distance from that point, whereas in the arc-length continuation, the scalar equation is that of an hypersphere centred at the operating point of the response curve and of a determined radius. During the correction phase, in the arc-length continuation method, the solution curve and the hypersphere always have more than one intersection point, whereas in the pseudo arc-length continuation method, the hyperplane may have no intersection point with the solution curve (where it is in proximity to the critical points, generally a turning point). This drawback can be remedied by a decrease of the discretisation step. In this paper, the arc-length continuation method will be preferred to the pseudo arc-length method.

The conjunction of the SM with Continuation techniques that will be henceforth referred to as SM+C, has been frequently used for mechanical applications. For instance, Rigaud and Perret-Liaudet [102] investigated numerical dynamic responses of a preloaded vibro-impacting Hertzian contact under sinusoidal excitation through SM+C (more precisely arc-length continuation). In [103], a semi-analytical shooting technique associated with a continuation technique using a combination of several prediction/correction schemes is used to describe the periodic orbits and their bifurcations (period doubling, saddle node bifurcation) for the nonlinear oscillations of a driving diesel engine vacuum pump. In [104], a SM+C technique is applied to calculate the periodic response and to study the stability and bifurcations of a periodically excited non-conservative Multi DoFs system with strong local nonlinearities (13 DoFs flexible rotor supported on journal bearings). While ten years ago the use of continuation schemes in conjunction with the HBM appeared to be not as common in engineering applications as the SMs, this tendency has since changed and both are more or less equally used [105]. For example, Lewandowski [106,107] used the HBM, which is equivalent to Ritz-Galerkin method, in combination with the arc-length continuation method HBM+C to solve a set of algebraic equations describing the free and steady-state vibration of geometrically nonlinear structures. Furthermore, the stability analysis can be easily taken into account.

Recently, Kerschen *et al* pointed out with two companion papers [108,109], new perspectives on the practical computation of NNMs. Specifically, they highlighted the capability of numerical algorithms to easily compute NNMs of strongly nonlinear systems. Moreover, they proposed a new frequency-energy plot representation to be compared with time-frequency plots of the response of the nonlinear systems. In this way, they claim that this new perspectives on NNMs will help to extend experimental modal analysis to a practical nonlinear analysis based on force appropriation.

References

- [1] Le Pape, Y., Anthoine, A., Pegon, P., (2001); *Seismic assessment of masonry structures - Multi-scale numerical modelling, Historical Constructions*, Guimaraes P. Roca.
- [2] Anthoine, A., (1992); *In-plane behaviour of masonry: a literature review*. JRC-Ispra, EUR-Report No. 13840 EN.
- [3] Page, A.W., (1978); *Finite element model for masonry*. Journal of Structural Division, 104(ST8), pp. 1267-1285.
- [4] Lofti, H.R., Shing, P.B., (1994); *Interface model applied to fracture of masonry structures*. ASCE Journal of Structural Engineering, 120(1), pp. 63-81.
- [5] Baggio, C., Trovalusci, P., (1993); *Discrete models for jointed block masonry walls*. Proceedings of the 6th North American Masonry Conference, Philadelphia, USA.
- [6] Lourenco, P.B., Rots, J.G., (1997); *Multisurface interface model for analysis of masonry structures*. Journal of engineering mechanics, 123(7), pp. 660-668.
- [7] Giambanco, G., Rizzo, S., Spallino, R., (2001); *Numerical analysis of masonry structures via interface models*. Comput. Methods Appl. Mech. Engrg., 190, pp. 6493-6511.
- [8] Chetouane, B., Dubois, F., Vinches, M., Bohatier, C., (2005); *NSCD discrete element method for modelling masonry structures*. International Journal for Numerical Methods in Engineering, 65, pp. 65-94.
- [9] Pietruszczak, S., Niu, X., (1992); *A mathematical description of macroscopic behaviour of brick masonry*. International Journal of Solids and Structures, 29(5), pp. 531-546.
- [10] Maier, G., Nappi, A., Papa, E., (1991); *Damage model for masonry as a composite material: a numerical and experimental analysis*. Proceedings of the 3rd International Conference on Constitutive laws for engineering materials: theory and application, Tucson, USA, pp. 427-432.
- [11] Alpa, G., Monetto, I., (1994); *Microstructural model for dry block masonry walls with in-plane loading*. Journal of the mechanics and physics of solids, 42(7), pp. 1159-1175.
- [12] De Buhan, P., De Felice, G., (1997); *A homogenization approach to the ultimate strength of brick masonry*. J. Mech. Phys. Solids, 45(7), pp. 1085-1104.
- [13] Luciano, R., Sacco, E., (1997); *Homogenization technique and damage model for old masonry material*. Int. J. Solids Structures, 34(24), pp. 3191-3208.
- [14] Sacco, E., (2009); *A nonlinear homogenization procedure for periodic masonry*. European Journal of Mechanics A/Solids, 28, pp. 209-222, doi: <http://dx.doi.org/10.1016/j.euromechsol.2008.06.005>.
- [15] Lourenco, P.B., De Borst, R., Rots, J.G., (1997); *A plane stress softening plasticity model for orthotropic materials*. International Journal for Numerical Methods in Engineering, 40, pp. 4033-4057.
- [16] Gambarotta, L., Lagomarsino, S., (1997); *Damage models for the seismic response of*

- brick masonry shear walls. Part I: the mortar joint model and its application.* Earthquake engineering and structural dynamics, 26, pp. 423-439.
- [17] Gambarotta, L., Lagomarsino, S., (1997); *Damage models for the seismic response of brick masonry shear walls. Part II: the continuum model and its applications.* Earthquake Engineering and Structural Dynamics, 26, pp. 441-462.
- [18] Calderini, C., Lagomarsino, S., (2008); *Continuum model for in-plane anisotropic inelastic behavior of masonry.* ASCE Journal of Structural Engineering, 134(2), p. 209.
- [19] Calderini, C., Lagomarsino, S., (2006); *A micromechanical inelastic model for historic masonry.* Journal of Earthquake Engineering, 10(4), pp. 453-479.
- [20] Cluni, F., Gusella, V., (2004); *Homogenization of non-periodic masonry structures.* International Journal of Solids and Structures, 41, pp. 1911-1923.
- [21] Massart, T.J., Peerlings, R.H.J., Geers, M.G.D., (2004); *Mesosopic modeling of failure and damage-induced anisotropy in brick masonry.* European Journal of Mechanics - A/Solids, 23, pp. 719-735.
- [22] Wu, C., Hao, H., (2006); *Derivation of 3D masonry properties using numerical homogenization technique.* International Journal for numerical methods in engineering, 66, pp. 1717-1737, doi: [10.1002/nme.1537](https://doi.org/10.1002/nme.1537).
- [23] Quinteros, R.D., Oller, S., Nallim, L.G., (2012); *Nonlinear homogenization techniques to solve masonry structures problems.* Composite Structures, 94, pp. 724-730, doi: <http://dx.doi.org/10.1016/j.compstruct.2011.09.006>.
- [24] Lopez, J., Oller, S., Onate, E., Lubliner, J., (1999); *A homogeneous constitutive model for masonry.* International Journal for Numerical methods in engineering, 46, pp. 1651-1671.
- [25] Cecchi, A., Sab, K., (2007); *A homogenized Reissner-Mindlin model for orthotropic periodic plates: Application to brickwork panels.* International Journal of Solid and Structures, 6055-6079, p. 44.
- [26] Caillerie, D., (1984); *Thin elastic and periodic plates.* Math. Method Appl. Science, 6, pp. 159-191.
- [27] Cecchi, A., Sab, K., (2009); *Discrete and continuous models for in plane loaded random elastic brickwork.* European Journal of Mechanics A/Solids, 28, pp. 610-625.
- [28] Cecchi, A., Sab, K., (2004); *A comparison between a 3D discrete model and two homogenised plate models for a periodic elastic brickwork.* International Journal of Solids and Structures, 41(9-10), pp. 2259-2276.
- [29] Andreaus, U., (1996); *Failure criteria for masonry panels under in-plane loading.* Journal of Structural Engineering, 122(37), pp. 37-46, doi: [10.1061/\(ASCE\)0733-9445\(1996\)122:1\(37\)](https://doi.org/10.1061/(ASCE)0733-9445(1996)122:1(37)).
- [30] Caughey, T.K., (1960); *Random excitation of a system with bilinear hysteresis.* Journal of Applied Mechanics, 27(4), pp. 649-652.
- [31] Caughey, T.K., (1960); *Sinusoidal excitation of a system with bilinear hysteresis.* Journal of Applied Mechanics, 27(4), pp. 640-643.
- [32] Iwan, W.D., (1965); *The steady-state response of a two-degree-of-freedom bilinear*

- hysteretic system*. Journal of Applied Mechanics, 32, pp. 151-156.
- [33] Masri, S.F., (1975); *Forced vibration of the damped bilinear hysteretic oscillator*. Journal of the Acoustic Society Am., 57, p. 106.
- [34] Pratap, R., Mukherjee, S., Moon, F.C., (1994); *Dynamic behavior of a bilinear hysteretic elasto-plastic oscillator. Part 1: Free oscillations*. Journal of Sound and Vibrations, 172(3), pp. 321-337.
- [35] Iwan, W.D., Asano, K., (1984); *An alternative approach to the random response of bilinear hysteretic systems*. Earthquake Engineering & Structural Dynamics, 12(2), pp. 229-236, doi: [10.1002/eqe.4290120207](https://doi.org/10.1002/eqe.4290120207).
- [36] Ibarra, L.F., Medina, R.A., Krawinkler, H., (2005); *Hysteretic models that incorporate strength and stiffness deterioration*. Earthquake Engineering and Structural Dynamics, 34, pp. 1489-1511, doi: [10.1002/eqe.495](https://doi.org/10.1002/eqe.495).
- [37] Clough, R.W., Johnston, S.B., (1966); *Effect of stiffness degradation on earthquake ductility requirements*. Proceedings of Japan Earthquake Engineering Symposium, Tokyo, pp. 227-232.
- [38] Cifuentes, A., (1984); *System identification of hysteretic structures*. California Institute of Technology, Pasadena, CA PhD Thesis.
- [39] Takeda, T., Sozen, M.A., Nielsen, N.N., (1970); *Reinforced Concrete Response to Simulated Earthquakes*. ASCE Journal of the Structural Division, 96(ST12), pp. 2557-2573.
- [40] Otani, S., (1974); *SAKE, A computer program for inelastic response of R/C Frames to Earthquakes*. University of Illinois, Urbana-Champaign Report UILU-Eng-74-2029.
- [41] Saiidi, M., Sozen, M.A., (1979); *Simple and Complex Models for Nonlinear Seismic Response of Reinforced Concrete Structures*. University of Illinois, Urbana Report No. UILU-ENG-79-2013.
- [42] Iwan, W.D., Cifuentes, A.O., (1986); *A model for system identification of degrading structures*. Earthquake Engineering & Structural Dynamics, 14, pp. 877-890.
- [43] Iwan, W.D., (1967); *On a Class of Models for the Yielding Behavior of Continuous and Composite Systems*. ASME Journal of Applied Mechanics, 34(3), pp. 612-617.
- [44] Masing, G., (1926); *Eigenspannungen und verfestigung beim messing (Self stretching and hardening for brass)*. Proceedings of 2nd International Congress for Applied Mechanics, Zurich, pp. 332-335.
- [45] Ashrafi, S.A., Smyth, A.W., (2007); *Generalized Masing approach to modeling hysteretic deteriorating behavior*. ASCE Journal of Engineering Mechanics, 133(5), p. 495.
- [46] Jayakumar, P., (1987); *Modeling and identification in structural dynamics*. California Institute of Technology, Pasadena Report No. eerl 87-01, PhD dissertation.
- [47] Vucetic, M., (1990); *Normalized behavior of clay under irregular cyclic loading*. Canadian Geotechnical Journal, 27(1), pp. 29-46.
- [48] Thyagarajan, R.S., (1990); *Modeling and analysis of hysteretic structural behaviour*. California Institute of Technology, Pasadena Report No. EERL 89-03, PhD

dissertation.

- [49] Chiang, D.Y., (1992); *Parsimonious modeling of inelastic systems*. California Institute of Technology, Pasadena Report No. EERL 92-02, PhD dissertation.
- [50] Ramberg, W., Osgood, W.R., (1943); *Description of Stress-Strain Curves by Three Parameters*. National Advisory Committee on Aeronautics, Technical Note No. 902.
- [51] Jennings, P.C., (1963); *Response of simple yielding structures to earthquake excitation*. California Institute of Technology, Pasadena PhD dissertation.
- [52] Matzen, V.C., McNiven, H.D., (1976); *Investigation of the Inelastic Characteristics of a Single Story Steel Structure using System Identification and Shaking Table Experiments*. Earthquake Engineering Research Center, University of California, Berkeley Report No. EERC 72-20.
- [53] Bouc, R., (1971); *Modèle mathématique d'hystérésis*. *Acustica*, 24, pp. 16-25.
- [54] Wen, Y.K., (1976); *Method of random vibration of hysteretic systems*. *ASCE J. of Eng. Mech.*, 102, pp. 249-263.
- [55] Heine, C.P., (2001); *Simulated response of degrading hysteretic joints with slack behaviour*. Virginia Polytechnic Institute and State University, Blacksburg, Virginia PhD Thesis.
- [56] Baber, T.T., Wen, Y.K., (1980); *Stochastic Equivalent Linearization for Hysteretic, Degrading, Multistory Structures*. University of Illinois, Urbana-Champaign Report No. 471 UILU-ENG-80-2001.
- [57] Erlicher, S., Point, N., (2004); *Thermodynamic admissibility of Bouc-Wen-type hysteresis models*. *Comptes Rendus Mécanique*, 332(1).
- [58] Erlicher, S., Point, N., (2006); *Endochronic theory, non-linear kinematic hardening rule and generalized plasticity: a new interpretation based on a generalized normality assumption*. *International Journal of Solids and Structures*, 43(14-15), pp. 4175-4200.
- [59] Erlicher, S., Bursi, O.S., (2007); *Bouc-Wen-type models with stiffness degradation: thermodynamic analysis and applications*. *ASCE Journal of Engineering Mechanics*.
- [60] Baber, T.T., Wen, Y.K., (1981); *Random vibrations on hysteretic, degrading systems*. *J. of Eng. Mech. Div.*, 107(6), pp. 1069-1087.
- [61] Wen, Y.K., (1980); *Equivalent Linearization for Hysteretic System under Random excitation*. *Journal of Applied Mechanics*, 47, pp. 150-154.
- [62] Baber, T.T., Noori, M.N., (1985); *Random vibration of degrading pinching systems*. *J. of Eng. Mech.*, 111(8), pp. 1010-1026.
- [63] Foliente, G.C., (1995); *Hysteresis Modeling of Wood Joints and Structural Systems*. *J. Struct. Engineering*, 121(6), pp. 1013-1022.
- [64] Sivaselvan, M.V., Reinhorn, A.M., (2000); *Hysteretic models for deteriorating inelastic structures*. *Journal of Engineering Mechanics*, 126, pp. 633-640.
- [65] Li, S.J., Suzuki, Y., Noori, M., (2004); *Identification of hysteretic systems with slip using bootstrap filter*. *Mech. Sys. and Signal Process.*, 18(4), pp. 781-795.
- [66] Ceravolo, R., Zanotti Fragonara, L., Erlicher, S., Bursi, O.S., (2011); *Parametric*

- identification of damaged dynamic systems with hysteresis and slip*. Journal of Physics: Conference Series, 305, pp. 1-10, doi: [10.1088/1742-6596/305/1/012050](https://doi.org/10.1088/1742-6596/305/1/012050).
- [67] Bursi, O.S., Ceravolo, R., Erlicher, S., Zanotti Fragonara, L., (2012); *Identification of the hysteretic behaviour of a partial-strength steel-concrete moment-resisting frame structure subject to pseudodynamic tests*. Earthquake Engineering & Structural Dynamics, In press.
- [68] Sivaselvan, M.V., Reinhorn, A.M., (2000); *Hysteretic Models for Deteriorating Inelastic Structures*. J. of Engineering Mechanics, 126(6), pp. 633-640.
- [69] Ikhoulane, F., Mañosa, V., Rodellar, J., (2007); *Dynamic properties of the hysteretic Bouc-Wen model*. Systems & Control Letters, 56, pp. 197-205.
- [70] Erlicher, S., Point, N., (2008); *Pseudo potentials and loading surfaces for an endochronic plasticity theory with isotropic damage*. J. of Engrg. Mech., 134(10), pp. 832-842.
- [71] Erlicher, S., Bursi, O.S., (2008); *Bouc-Wen-type models with stiffness degradation: thermodynamic analysis and applications*. J. of Eng. Mech., 134(10), pp. 843-855.
- [72] Chen, W.-F., Ting, E.C., (1980); *Constitutive Models for Concrete Structures*. ASCE Journal of the Engineering Mechanics Division, 106(1), pp. 1-19.
- [73] Sandler, I.S., (1978); *On the uniqueness and stability of Endochronic theories of material behavior*. ASME Journal of Applied Mechanics, 45(2), pp. 263-266.
- [74] Pesheck, E., Pierre, C., Shaw, S.W., (2001); *Accurate reduced order models for a simple rotor blade model using nonlinear normal modes*. Math. Comput. Model, 33, pp. 1085-97.
- [75] Apiwattanalungarn, P., Shaw, S.W., Pierre, C., (2005); *Component mode synthesis using nonlinear normal modes*. Nonlinear Dynamics, 41, pp. 17-46.
- [76] Rosenberg, R.M., (1966); *On nonlinear vibrations of systems with many degrees of freedom*. Advanced Applied Mechanics, 9, pp. 155-242.
- [77] Lyapunov, A., (1947); *The general problem of the stability of motion*. Annal of Math. Studies, 17.
- [78] Vakakis, A.F., (1997); *Non-linear normal modes (NNMs) and their applications in vibration theory: an overview*. Mechanical Systems and Signal Processing, 11(1), pp. 3-22.
- [79] Vakakis, A.F., Manevitch, L.I., Philipchuck, Y.V., Zevin, A.A., (1996); *Normal Modes and localization in nonlinear systems*, Wiley interscience.
- [80] Li, X., Ji, J.C., Hansen, C.H., (2006); *Non-linear normal modes and their bifurcation of two DOF system with quadratic and cubic non-linearity*. International Journal of Non-Linear Mechanics, 41(9), pp. 1036-46.
- [81] Szemplinska-Stupnicka, W., (1991); *Analysis of nonlinear dynamical systems by the normal form theory*. Journal of Sound and Vibration, 149(3), pp. 429-459.
- [82] Jézéquel, L., Lamarque, C.H., (1991); *Analysis of nonlinear dynamical systems by the normal form theory*. Journal of Sound and Vibrations, 149(3), pp. 429-459.
- [83] Shaw, S.W., Pierre, C., (1991); *Non-linear normal modes and invariant manifolds*. Journal of Sound and Vibration, 150(1), pp. 170-173.

- [84] Shaw, S.W., Pierre, C., (1993); *Normal modes of vibration for non-linear vibratory systems*. Journal of Sound and Vibrations, 164(1), pp. 85-124.
- [85] Guckenheimer, J., Holmes, P., (1983); *Nonlinear oscillations, dynamical systems, and bifurcations of vector fields*, New York Springer-Verlag.
- [86] Slater, J.C., Inman, D.J., (1997); *On the effect of weak non-linearities on linear controllability and observability norms, an invariant manifold approach*. Journal of Sound and Vibrations, 199(3), pp. 417-429.
- [87] Nayfeh, A.H., Nayfeh, S.A., (1994); *On nonlinear modes of continuous systems*. Journal Vib. Acoust., 116, pp. 129-136.
- [88] Nayfeh, A.H., Chin, C., Nayfeh, S.A., (1996); *On nonlinear normal modes of systems with internal resonance*. J. Vib. Acoust., 118, pp. 340-345.
- [89] Pescheck, E., Boivin, N., Pierre, C., Shaw, S.W., (2001); *Nonlinear modal analysis of structural systems using multi-mode invariant manifolds*. Nonlinear Dynamics, 25, pp. 183-205.
- [90] Pescheck, E., Pierre, C., Shaw, S.W., (2002); *A new Galerkin-based approach for accurate non-linear normal modes through invariant manifolds*. Journal of Sound and Vibrations, 249(5), pp. 971-993.
- [91] Jiang, D., Pierre, C., Shaw, S.W., (2004); *Large-amplitude nonlinear normal modes of piecewise linear systems*. Journal of Sound and Vibrations, 217(3), pp. 869-891.
- [92] Jiang, D., Pierre, C., Shaw, S.W., (2005); *The construction of non-linear normal modes for systems with internal resonance*. International Journal of Non-linear mechanics, 40, pp. 729-746.
- [93] Legrand, M., Jiang, D., Pierre, C., Shaw, S.W., (2004); *Nonlinear normal modes of a rotating shaft based on the invariant manifold method*. Int. J. Rotating Machinery, 10(4), pp. 319-335.
- [94] Jiang, D., Pierre, C., Shaw, S.W., (2005); *Non-linear normal modes for vibratory systems under harmonic excitation*. Journal of Sound and Vibrations, 288(4-5), pp. 791-812.
- [95] Bellizzi, S., R., B., (2005); *A new formulation for the existence and calculation of nonlinear normal modes*. Journal of Sound and Vibrations, 287(7), pp. 545-569.
- [96] Bellizzi, S., Bouc, R., (2004); *A new formulation for the existence and calculation of nonlinear modes*. Proceedings of Euromech 457 on nonlinear modes of vibrating systems.
- [97] Gudmunson, P., (1989); *On the accuracy of the harmonic balance method concerning vibrations of beams with nonlinear supports*. Ingenieur-Archiv, 59, pp. 333-344.
- [98] Stoer, J., Bulirsch, R., (1980); *Introduction to Numerical Analysis*, New York Springer-Verlag.
- [99] Keller, H.B., (1987); *Lectures on Numerical methods in bifurcation problems. Lectures on Mathematics and Physics, Tata Institute of Fundamental Research*, Springer-Verlag.
- [100] Seydel, R., (1988); *From equilibrium to chaos: practical bifurcation and stability analysis*, New York Elsevier Science.

- [101] Baguet, S., Cochelin, B., (2003); *On the behaviour of the ANM continuation in the presence of bifurcations*. Commun. Numer. Methods Eng., 19(6), pp. 459-471.
- [102] Rigaud, E., Pierret-Liaudet, J., (2003); *Experiments and numerical results on non-linear vibrations of an impacting Hertzian contact. Part 1: harmonic excitation*. Journal of Sound and Vibrations, 265, pp. 289-307.
- [103] Amado, T., Thouverez, F., Dimitrijevic, Z., Dubost, J., (2004); *Nonlinear dynamics of a vacuum pump driving*. Proceedings of Euromech 457 on nonlinear modes of vibrating systems, pp. 187-190.
- [104] Sundararajan, P., Noah, S.T., (1998); *An algorithm for response and stability of large order non-linear systems - Application to rotor systems*. Journal of Sound and Vibrations, 214(4), pp. 695-723.
- [105] Von Groll, G., Ewins, D.J., (2001); *The harmonic balance method with arc-length continuation in rotor/stator contact problems*. Journal of Sound and Vibrations, 241(2), pp. 223-233.
- [106] Lewandowski, R., (1997); *Computational formulation for periodic vibration of geometric nonlinear structures, Part 1: theoretical background*. Int. Journal of Solids Struct., 34(15), pp. 1925-47.
- [107] Lewandowski, R., (1997); *Computational formulation for periodic vibration of geometric nonlinear structures, Part 2: numerical strategy and examples*. Int. Journal of Solids Struct., 34(15), pp. 1949-64.
- [108] Kerschen, G., Peeters, M., Golinval, J.C., Vakakis, A.F., (2009); *Nonlinear normal modes, Part I: A useful framework for the structural dynamicist*. Mechanical Systems and Signal Processing, 23, pp. 170-194.
- [109] Peeters, M., Vigiúé, R., Sérandour, G., Kerschen, G., Golinval, J.-C., (2009); *Nonlinear normal modes, Part II: Toward a practical computation using numerical continuation techniques*. Mechanical Systems and Signal Processing, 23, pp. 195-216.

